

The Chevron Effect and Analysis of Chevron Beams— A Paradigm Shift

PATRICK J. FORTNEY and WILLIAM A. THORNTON

ABSTRACT

Beam designers and connection designers have a different standard of care in the analysis of beams in inverted V- and V-type braced frames subjected to lateral loads. When the summation of the vertical components of the brace forces is nonzero, (1) beam designers evaluate required beam shear and moment, treating the unbalanced vertical load as a concentrated force acting at the work point of the braces while ignoring any local effects resulting from the brace connection geometry, and (2) the connection designer evaluates the required beam shear based only on the moment acting at the gusset-to-beam interface(s). Thus, the beam designer considers beam span and work point location, ignoring the local effect of the connection, and the connection designer considers the local effects of the connection while ignoring beam span and the location of the work point.

This paper proposes a new method for evaluating required beam shear and moment that includes consideration of beam span, location of work point, and the local effects of the connection—a method that can be used by both the beam designer and the connection designer. Discussion is also provided to illustrate how this proposed method can be used to evaluate whether or not the local connection effect dominates the global effect. It is shown that the magnitude of the unbalanced vertical load influences the impact of the local connection effects; when the summation of the vertical brace force components is zero or relatively small, the local connection effects dominate the global effect. Conversely, when the unbalanced vertical load is relatively large, the global effects dominate; in this case, including the local connection effects will predict a smaller required beam moment possibly allowing for lighter beams.

Keywords: chevron effect, braced frames, work point, V-type, inverted V-type, unbalanced vertical load.

INTRODUCTION

The presence of the gusset plate in a chevron brace connection imparts increases in beam shear and moment demand not captured by the analysis procedures currently used by beam designers and connection designers. This phenomenon was introduced by Fortney and Thornton (2015), who exposed the issue and made recommendations that beam designers could use to estimate connection geometry in an attempt to capture the chevron effect when sizing the frame beams. However, those recommendations were empirically based—more rules of thumb than approaches based on mechanics.

In this follow-on paper, the authors provide recommendations for an approach that can be used by both beam designers and connections designers; the approach is based on first principles and is given in the form of relatively easy-to-use, closed-form equations.

BRACE CONNECTION FORCE DISTRIBUTION

The force distribution in chevron brace connections where braces frame to the bottom side of the frame beam are derived by Fortney and Thornton (2015). For convenience, those equations are shown in Equations 1 through 10 and are supported with the free-body diagram (FBD) shown in Figure 1. Fortney and Thornton did not provide force distributions for braces framing to the top side of a frame beam. Those equations are given in Equations 11 through 19 and are supported in the FBD shown in Figure 1. Equations 11 through 19 were derived in a similar manner as that shown by Fortney and Thornton relative to bottom side braces.

SIGN CONVENTION

The sign convention used throughout this paper assumes that forces on gusset(s) acting to the right or upward, and clockwise moments acting on gusset(s), are positive.

FORCE AND MOMENT EQUATIONS

When the centroid of the gusset-to-beam interface is not horizontally aligned with the work point (see Figure 1), the parameter Δ can be calculated as

Patrick J. Fortney, Ph.D., P.E., S.E., PEng, Associate Professor, University of Cincinnati, Cincinnati, OH. Email: patrick.fortney@uc.edu (corresponding)

William A. Thornton, Ph.D., P.E., NAE, Cives Engineering Corporation, Roswell, GA. Email: bthornton@cives.com

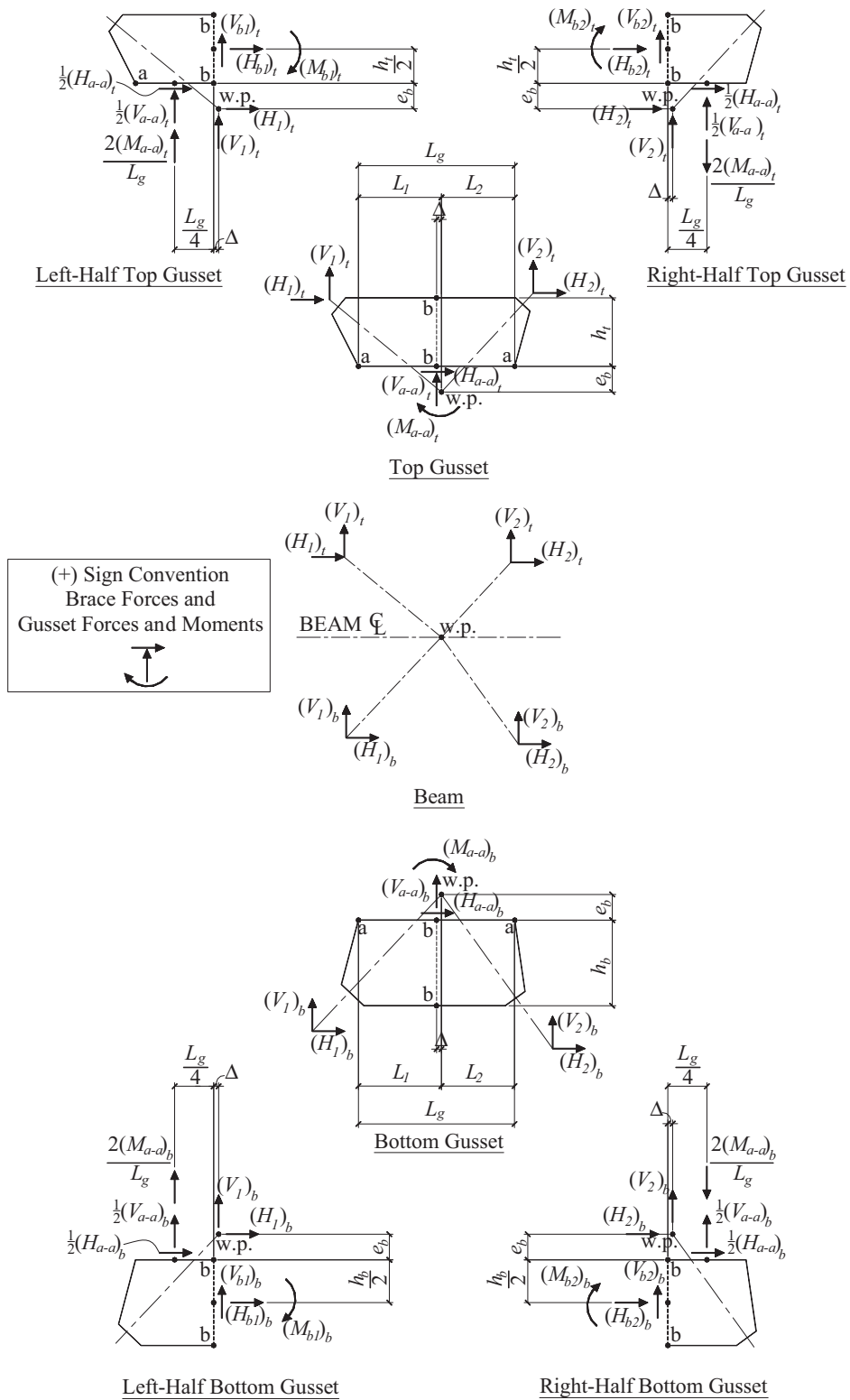


Fig. 1. FBD of force distribution in V-type and inverted V-type brace connections.

$$\Delta = \frac{1}{2}(L_1 - L_2) \quad (1)$$

Bottom Gusset

The forces and moment acting on the bottom gusset at section a-a are

$$(H_{a-a})_b = -(H_1 + H_2)_b \quad (2)$$

$$(V_{a-a})_b = -(V_1 + V_2)_b \quad (3)$$

$$(M_{a-a})_b = (V_1 + V_2)_b \Delta - (H_1 + H_2)_b e_b \quad (4)$$

The forces and moment acting on the bottom gusset at section b-b (left half of gusset) are

$$(H_{b1})_b = \frac{1}{2}(H_1 + H_2)_b - (H_1)_b \quad (5)$$

$$(V_{b1})_b = \frac{1}{2}(V_1 + V_2)_b - \frac{2(M_{a-a})_b}{L_g} - (V_1)_b \quad (6)$$

$$(M_{b1})_b = \frac{L_g}{8}(V_1 + V_2)_b + \frac{h_b}{4}(H_1 + H_2)_b - \frac{(M_{a-a})_b}{2} + \quad (7)$$

$$(V_1)_b \Delta - (H_1)_b \left(e_b + \frac{h_b}{2} \right)$$

The forces and moment acting on the bottom gusset at section b-b (right half of gusset) are

$$(H_{b2})_b = \frac{1}{2}(H_1 + H_2)_b - (H_2)_b \quad (8)$$

$$(V_{b2})_b = \frac{1}{2}(V_1 + V_2)_b + \frac{2(M_{a-a})_b}{L_g} - (V_2)_b \quad (9)$$

$$(M_{b2})_b = -\frac{L_g}{8}(V_1 + V_2)_b + \frac{h_b}{4}(H_1 + H_2)_b - \frac{(M_{a-a})_b}{2} +$$

$$(V_2)_b \Delta - (H_2)_b \left(e_b + \frac{h_b}{2} \right) \quad (10)$$

Note that the equations describing the forces and moment acting on the left half of the gusset on section b-b (Equations 5–7) give forces and moment equal to those forces and moment acting on the right half of the gusset on section b-b (Equations 8–10) but are opposite in sign.

TOP GUSSET

The forces and moments acting on the top gusset at section a-a are

$$(H_{a-a})_t = -(H_1 + H_2)_t \quad (11)$$

$$(V_{a-a})_t = -(V_1 + V_2)_t \quad (12)$$

$$(M_{a-a})_t = (H_1 + H_2)_t e_b + (V_1 + V_2)_t \Delta \quad (13)$$

The forces and moment acting on the top gusset at section b-b (left half of gusset) are

$$(H_{b1})_t = \frac{1}{2}(H_1 + H_2)_t - (H_1)_t \quad (14)$$

$$(V_{b1})_t = \frac{1}{2}(V_1 + V_2)_t - \frac{2(M_{a-a})_t}{L_g} - (V_1)_t \quad (15)$$

$$(M_{b1})_t = \frac{L_g}{8}(V_1 + V_2)_t - \frac{h_t}{4}(H_1 + H_2)_t - \frac{(M_{a-a})_t}{2} + \quad (16)$$

$$(V_1)_t \Delta + (H_1)_t \left(e_b + \frac{h_t}{2} \right)$$

The forces and moment acting on the top gusset at section b-b (right half of gusset) are

$$(H_{b2})_t = \frac{1}{2}(H_1 + H_2)_t - (H_2)_t \quad (17)$$

$$(V_{b2})_t = \frac{1}{2}(V_1 + V_2)_t + \frac{2(M_{a-a})_t}{L_g} - (V_2)_t \quad (18)$$

$$(M_{b2})_t = -\frac{L_g}{8}(V_1 + V_2)_t - \frac{h_t}{4}(H_1 + H_2)_t - \frac{(M_{a-a})_t}{2} + \quad (19)$$

$$(V_2)_t \Delta + (H_2)_t \left(e_b + \frac{h_t}{2} \right)$$

Note that the equations describing the forces and moment acting on the left half of the gusset on section b-b (Equations 14–16) give forces and moment equal to those forces and moment acting on the right half of the gusset on section b-b (Equations 17–19) but are opposite in sign.

THE CHEVRON EFFECT

When the summation of the vertical components of brace forces, $\sum V_i$, sum to zero, a beam analysis assuming a concentrated load acting transversely to the beam and located at the work point (referred to as a Pb/L , Pab/L analysis) will result in the beam having zero shear and zero moment. However, the presence of the brace connection imparts local shear and moment to the beam within the connection region. This local effect is referred to as the chevron effect (Fortney and Thornton, 2015). Under this loading, the beam end reactions and beam shear and moment outside of the connection region are zero. Figure 2 shows representative diagrams for beam shear and moment when $\sum V_i$ sum to zero.

A new proposed analysis method will be discussed in more detail later in this paper. The uniformly distributed loads and moment shown in Figure 2 are a fundamental assumption in that proposed analysis method.

DIVERGENT ANALYSES

The Beam Designer's Approach

Typically, designers charged with beam analysis and design (beam size selection) will evaluate required beam shear and flexural strength with an analysis that assumes that the $\sum V_i$ is a concentrated load that acts at the work point. Figure 3a shows a representative beam model and resulting beam shear and moment distribution for this loading assumption. This analysis takes into account the span of the beam and the location of the work point along the beam span, but it ignores the local effects of the brace connection, which can be significant as shown previously in Figure 2. Note that the loading in Figure 3a assumes that the brace tension load, P_1 , is larger than the brace compression load, P_2 . The sign of the beam shear and moment is dependent on the relative magnitudes of the brace tension and compression loads.

The Connection Designer's Approach

Conversely, connection designers will evaluate beam shear based on the moment that acts at the gusset-to-beam interface

and the required beam shear is $2M_{a-a}/L_g$ (the nonzero $\sum V_i$ is ignored altogether). Because the unbalanced vertical force is ignored by connection designers, beam shear and moment as well as beam end reactions are taken as zero. Figure 3b shows a representative beam model and resulting beam shear and moment distribution with this loading assumption. Typically, connection designers do not even evaluate required beam moment. However, to complete this type of analysis, the beam moment associated with this beam shear is $M_{a-a}/2$. With this type of analysis, connection designers consider the local effects of the connection but neglect the beam span and location of the work point and do not wholly consider the unbalanced vertical load. Additionally, because the beam shear is taken as the force couple of the moment, M_{a-a} , beam shear and moment are assumed to exist only within the middle half of the gusset length, L_g .

Comparison of the Two Approaches with the Chevron Effect

Figure 3 compares the divergent analyses performed by beam designers and connection designers. Note that the current standard of care performed by connection designers assumes concentrated forces that are the force couple of the moment, M_{a-a} , and act only within the middle half of the gusset length—unlike the uniformly distributed loads that are assumed when generating the beam shear and moments shown in Figure 2, where the loads are distributed along

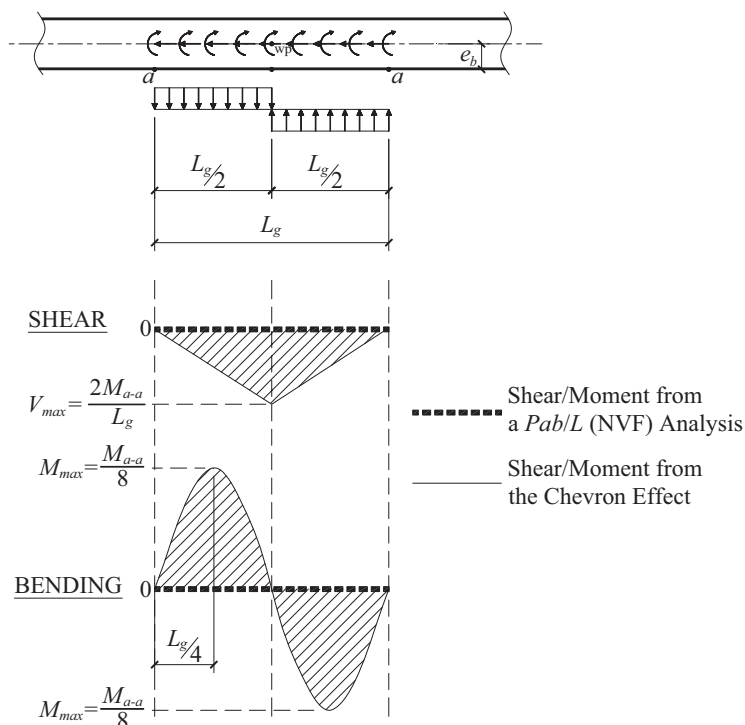
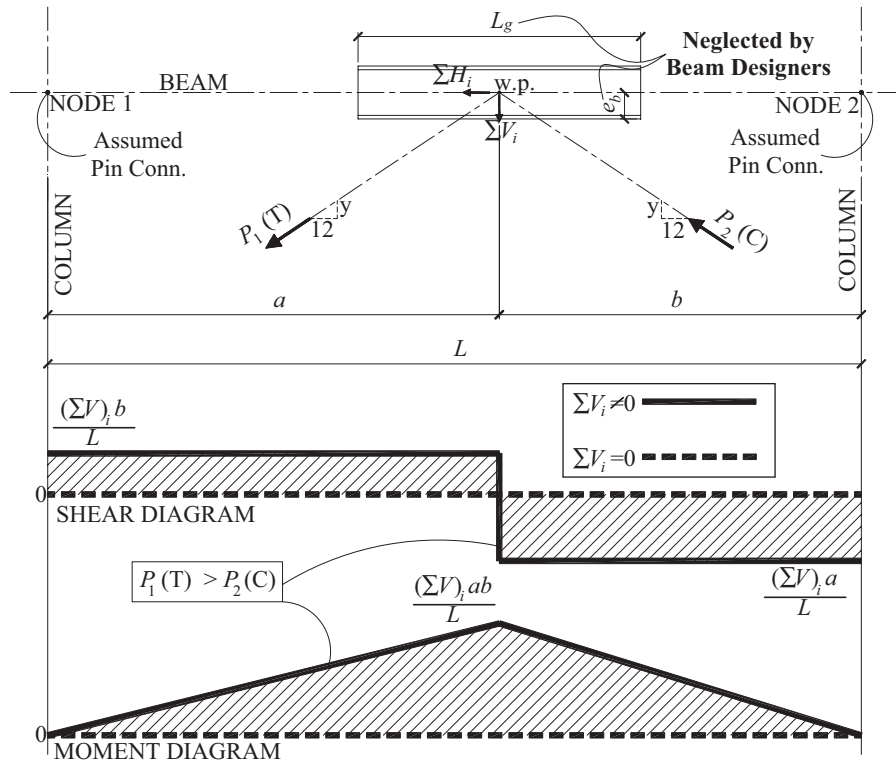
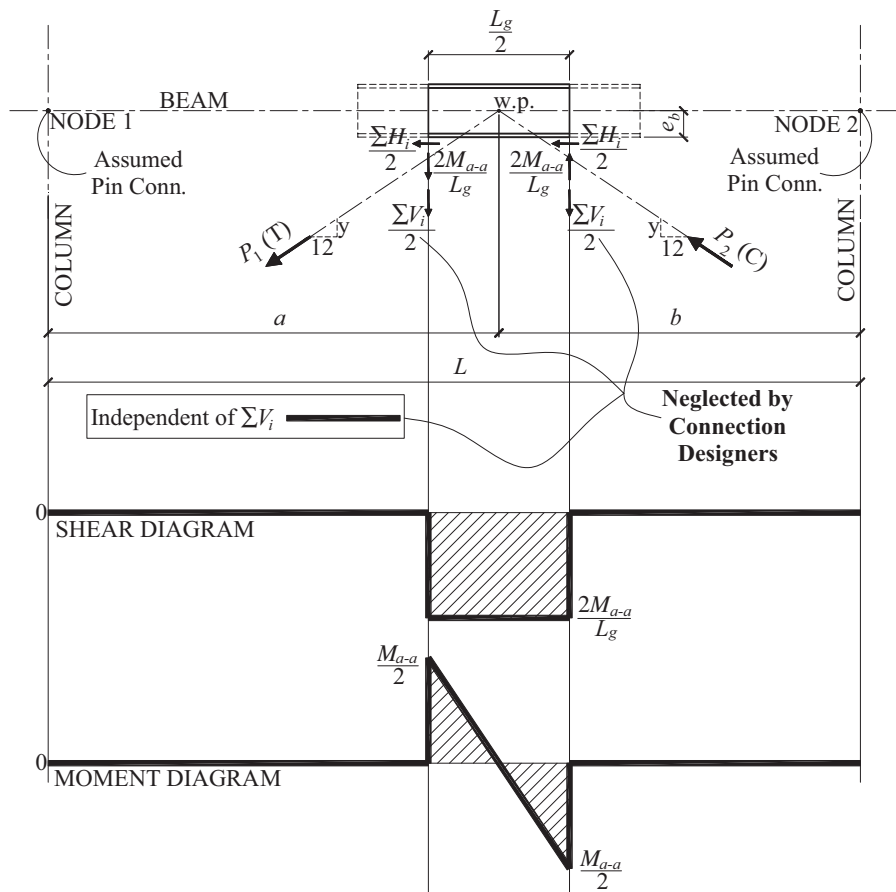


Fig. 2. Representation of the chevron effect; $(\sum V_i) = 0$.



(a) Beam designer analysis; span and work point considered; local effects ignored



(b) Connection designer analysis; span and work point ignored; local effects considered

Fig. 3. Comparison of analysis performed by beam and connection designers. (Note: Δ is assumed to be zero in these figures.)

the entire gusset length. Note that the maximum beam shear is the same for either case. However, the maximum beam moment when assuming uniformly distributed loads as shown in Figure 2 is one-fourth of that when assuming concentrated loads as shown in Figure 3 (recall that beam shear and moment using the current connection designer's approach is independent of the unbalanced vertical load).

As discussed previously, the beam designer's approach neglects the brace connection geometry, thereby neglecting the chevron effect altogether.

As one might expect, the required beam shears and moments determined from the two different procedures (i.e., beam designer versus connection designer) vary drastically. The following discussion attempts to address this issue and propose an analysis procedure that synergizes the analysis performed by beam designers and connection designers such that both individual approaches arrive at the same solution.

SYMBIOTIC ANALYSIS MODEL

The objective for a common method is to develop a procedure that can be used by both beam designers and connection designers, with both arriving at the same required beam shear and moment. The method accounts for beam span, location of work point, and connection geometry. In that there are virtually an infinite number of different possible connection geometries, the method presented here makes the following simplifying assumptions:

- Only lateral load is considered to focus on the issue; in real design, the combination of other applicable loads will need to be carefully considered.
- When braces frame to both the top and bottom flanges,
 - Gusset lengths, L_g , at top and bottom are the same.
 - The vertical edges of the top and bottom gussets are horizontally aligned.

Note that with these two assumptions, the Δ term will be the same for the top and bottom gussets.

- The unbalanced vertical force(s), ΣV_i , is distributed uniformly along the interface(s), L_g .
- The moment(s), M_{a-a} , is distributed uniformly along the interface(s) using a plastic distribution.
- The moment(s) needed to transport the summation of the horizontal forces acting at the interface(s) to the gravity axis of the beam is applied as a uniformly distributed moment, q , over the interface length, L_g .

The Beam Model

The following equations used to evaluate required beam shear and moment are consistent with the sign convention used to derive the equations describing the connection force distributions given in Equations 1 through 19. Refer to the "Sign Convention" section.

The chevron effect does not produce beam end reactions; end reactions are only a function of the unbalanced load, $(\Sigma V)_T$, beam span, L , and location of the work point along the span of the beam, a . Thus, the left beam end reaction, R_1 , shown in Figures 4 and 5 is as given in Equation 20:

$$R_1 = \frac{-(\Sigma V)_T b}{L} \quad (20)$$

where

$$(\Sigma V)_T = (\Sigma V)_t + (\Sigma V)_b \quad (21)$$

In Equation 21, the subscripts t and b represent forces acting on the top and bottom sides of the beam, respectively.

The uniformly distributed loads acting on the beam, w_t and w_b , shown in Figures 4 and 5 are the net transverse loads from both the unbalanced vertical force(s), $(\Sigma V)_T$, and the interface moment(s), M_{a-a} , distributed as a plastic moment

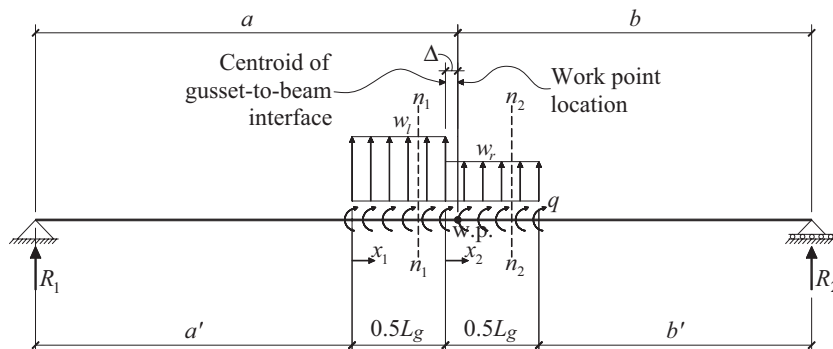


Fig. 4. Beam model; see Fig. 5 for FBDs.

uniformly over the left and right halves of the gussets, respectively, and are calculated as

$$w_l = -\left(\frac{4M_{a-a}}{L_g^2}\right)_t - \left(\frac{4M_{a-a}}{L_g^2}\right)_b + \left(\frac{\sum V}{L_g}\right)_t + \left(\frac{\sum V}{L_g}\right)_b \quad (22)$$

$$w_r = \left(\frac{4M_{a-a}}{L_g^2}\right)_t + \left(\frac{4M_{a-a}}{L_g^2}\right)_b + \left(\frac{\sum V}{L_g}\right)_t + \left(\frac{\sum V}{L_g}\right)_b \quad (23)$$

The third and fourth terms shown in Equations 22 and 23 can be simplified in terms of the total unbalanced vertical force, $(\sum V)_T$, as

$$\left(\frac{\sum V}{L_g}\right)_T = \left(\frac{\sum V}{L_g}\right)_t + \left(\frac{\sum V}{L_g}\right)_b \quad (24)$$

The uniformly distributed moment, q , shown in Figures 4 and 5, is the sum of the horizontal loads acting at the gusset-to-beam interface(s) multiplied by one-half the depth of the beam, e_b , and divided by the gusset length L_g , and is given in Equation 25:

$$q = \left[(\sum H)_t - (\sum H)_b \right] \left(\frac{e_b}{L_g} \right) \quad (25)$$

Maximum Beam Shear and Moment in the Left Half of the Gusset

When the magnitude of the tension brace force is larger than the magnitude of the compression brace force and the left brace and right braces are in tension and compression, respectively, the direction of the distributed moment, q , will be positive (clockwise). Under this type of loading, the maximum beam moment will occur somewhere between the left edge of the gusset(s) and mid-length of the gusset(s), $L_g/2$. The FBD shown in Figure 5a can be used to write equations that describe the distribution of beam shear and moment along the span of the beam.

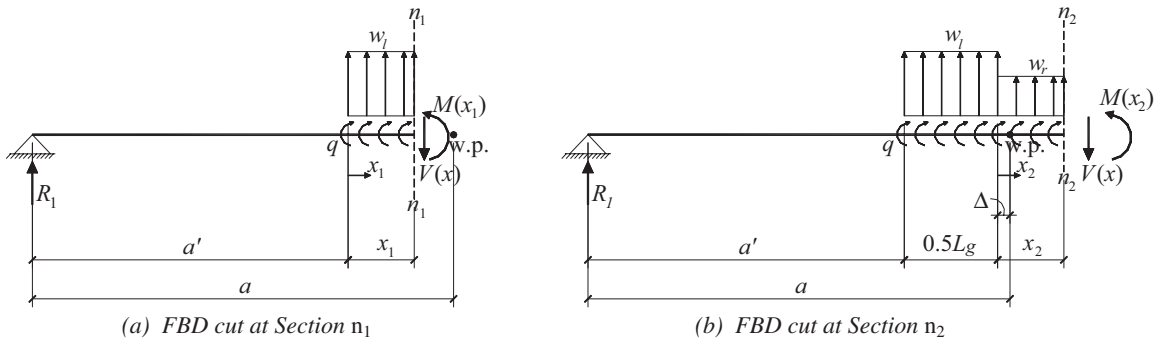


Fig. 5. FBDs used to write beam shear and moment equations; see Fig. 4 for beam model.

The moment distribution, $M(x_1)$, is

$$M(x_1) = R_1 a' + R_1 x_1 + 0.5 w_l x_1^2 + q x_1 \quad (26)$$

To locate where the maximum moment occurs, the derivative of Equation 26 is taken and set equal to zero:

$$\frac{d}{dx_1} M(x_1) = 0 = R_1 + w_l x_1 + q \quad (27)$$

Solving Equation 27 for x_1 , the maximum moment occurs a distance from the left edge of the gusset at

$$x_1 = \frac{-R_1 - q}{w_l} \quad (28)$$

where x_1 is valid for a range of

$$0 \leq x_1 \leq \frac{L_g}{2} \quad (29)$$

Substituting Equation 28 into Equation 26 gives the equation for maximum beam moment:

$$M_{\max} = \underbrace{\frac{R_1 a'}{Pab/L} + (R_1 + q)}_{\text{Effect of Gusset}} \left(\frac{-R_1 - q}{w_l} \right) + 0.5 w_l \left(\frac{-R_1 - q}{w_l} \right)^2 \quad (30)$$

To ensure that Equation 30 gives maximum and not minimum moment, the second derivative of Equation 26 is taken. The second derivative is

$$\frac{d^2}{dx_1^2} M(x_1) = w_l \quad (31)$$

When w_l is negative (acting downward), Equation 30 gives a maximum moment in the x_1 region when the moment is positive and gives a minimum moment when the moment is negative. When w_l is positive (acting upward), Equation 30 gives a minimum moment in the x_1 region when the moment is positive and a maximum moment when the moment is

negative. In either case, it is best to check the x_2 region (see Figure 5b) and compare the results to determine the overall maximum moment as the maximum beam moment may occur in the beam along the region of the right half of the gusset(s). The equations for the x_2 region (right half of gusset) are presented in the next section of this paper.

The beam shear is distributed over the span of the beam, $V(x_1)$, as given by Equation 32:

$$V(x_1) = \underbrace{R_1}_{\text{Pb/L Analysis}} + \underbrace{w_l x_1}_{\text{Effect of Gusset}} \quad (32)$$

In most cases, the maximum beam shear occurs at mid-length of the gusset, $L_g/2$. In rare cases, the net uniformly distributed loads, w_l and w_r , can be the same sign (i.e., both acting downward or both acting upward). In these rare cases, the magnitude of the uniformly distributed plastic moment is smaller than the magnitude of the uniformly distributed unbalanced vertical load. So for most cases, when the magnitude of the plastic moment distribution exceeds the magnitude of the uniformly distributed unbalanced vertical load, the maximum shear can be calculated by substituting $L_g/2$ for the x_1 :

$$V_{max} = R_1 + 0.5w_l L_g \quad (33)$$

Maximum Shear and Moment in Right Half of Gusset

When the magnitude of the tension brace force is larger than the magnitude of the compression brace force and the left brace and right braces are in compression and tension, respectively, the direction of the distributed moment, q , will be negative (counterclockwise). Under this type of loading, the maximum beam moment will occur somewhere between the mid-length of the gusset(s), $L_g/2$ and the right edge of the gusset(s). The FBD shown in Figure 5b can be used to write equations that describe the distribution of beam shear and moment along the span of the beam.

The moment distribution, $M(x_2)$, is

$$M(x_2) = 0.5w_r x_2^2 + (R_1 + 0.5w_l L_g + q)x_2 + R_1(a' + 0.5L_g) + 0.125w_l L_g^2 + 0.5qL_g \quad (34)$$

To locate where the maximum moment occurs, the derivative of Equation 34 is taken and set equal to zero:

$$\frac{d}{dx_2} M(x_2) = 0 = R_1 + 0.5w_l L_g + q + w_r x_2 \quad (35)$$

Solving Equation 35 for x_2 , the maximum moment occurs a distance from the mid-length of the gusset at

$$x_2 = -\frac{R_1 + 0.5w_l L_g + q}{w_r} \quad (36)$$

where x_2 is valid for a range of

$$0 \leq x_2 \leq \frac{L_g}{2} \quad (37)$$

Substituting Equation 36 into Equation 34 gives the equation for maximum beam moment:

$$M(x_2) = 0.5w_r \left(-\frac{R_1 + 0.5w_l L_g + q}{w_r} \right)^2 + (R_1 + 0.5w_l L_g + q) \left(-\frac{R_1 + 0.5w_l L_g + q}{w_r} \right) + R_1(a' + 0.5L_g) + 0.125w_l L_g^2 + 0.5qL_g \quad (38)$$

To ensure that Equation 38 gives maximum moment, and not minimum moment, the second derivate of Equation 34 is taken. The second derivative is

$$\frac{d^2}{dx_2^2} M(x_2) = w_r \quad (39)$$

When w_r is negative (acting downward), Equation 38 gives a maximum moment in the x_2 region when the moment is positive and a minimum moment when the moment is negative. When w_r is positive (acting upward), Equation 38 gives a minimum moment when the moment is positive and a maximum moment when the moment is negative. As stated previously, it is good practice to evaluate moments in both the x_1 and x_2 regions to determine the overall maximum moment.

The beam shear is distributed over the span of the beam, $V(x_2)$, as given by Equation 40:

$$V(x_2) = \underbrace{R_1}_{\text{Pb/L Analysis}} + \underbrace{0.5w_l L_g + w_r x_2}_{\text{Effect of Gusset}} \quad (40)$$

In most cases, the maximum beam shear occurs at mid-length of the gusset, $L_g/2$. In rare cases, the net uniformly distributed loads, w_1 and w_2 , can be the same sign (i.e., either both acting downward or both acting upward). In these rare cases, the magnitude of the uniformly distributed plastic moment is smaller than the magnitude of the uniformly distributed unbalanced vertical load. And for the majority of cases, when the magnitude of the plastic moment distribution exceeds the magnitude of the uniformly distributed unbalanced vertical load, the maximum shear can be calculated by substituting $x_2 = 0$ for x_2 . Note that this gives the same maximum shear as given in Equation 33:

$$V_{max} = R_1 + 0.5w_l L_g \quad (41)$$

Rule of Thumb for Connection Geometry

In order for the beam designer to use the proposed equations, the length of the gusset, L_g , and the depth of the beam, $2e_b$, would need to be known. Typically, the brace connection geometry is not known by the beam designer at the time the beam size is selected. Fortney and Thornton (2015)

recommend an approximated gusset length, $L_{g,app}$, equal to

$$L_{g,app} = \frac{L}{6} \quad (42)$$

and an approximated half beam depth, $e_{b,app}$, in in., equal to

$$e_{b,app} = 0.375 \text{ (span of beam in feet)} \quad (43)$$

EVALUATING THE CHEVRON EFFECT

Does the Chevron Effect Dominate?

There are many ways the chevron effect can be evaluated. Two methods are presented here:

1. For a given condition (i.e., the beam span, work point location, and unbalanced vertical force are known), an equivalent gusset length is calculated and compared to the provided gusset length to determine if the chevron effect will dominate—a method that will be useful to the connection designer.
2. For a known beam span, L , an approximated gusset length, $L_{g,app}$, and an approximated half beam depth, $e_{b,app}$, an equivalent unbalanced vertical force can be calculated and compared to the actual unbalanced vertical force to determine if the chevron effect will dominate—a method that will be useful to beam designers.

The equations shown for the following two methods assume that the maximum beam moment occurs in the left half of the gusset. For a specific case where the maximum beam moment occurs in the right half of the gusset, the equations presented can be used by reversing the brace loads.

Comparison of Gusset Lengths, L_g

Figure 6 shows representative beam shear and moment diagrams that consider the local effect as well as the unbalanced vertical loads (brace loads). The maximum moment occurs somewhere between the left edge and the middle of the gusset at a distance, x , from the left edge of the gusset. The change in moment, ΔM_{local} , considering the local effects is

$$\Delta M_{local} = 0.5w_l x^2 + (R_1 + q)x \quad (44)$$

where R_1 is given in Equation 20, w_l is given by Equation 22, and q is given in Equation 25.

Figure 6b shows representative beam shear and moment diagrams that consider only the unbalanced vertical load effect (brace loads). The maximum moment, $M_{max,unbal}$, occurs at the mid-point, which, for this discussion, is considered to be located at mid-length of the gusset (i.e., at $L_g/2$ from the left edge of the gusset). Thus, the change in moment, ΔM_{unbal} , from the left edge of the gusset to mid-length of the gusset is

$$\Delta M_{unbal} = R_1(0.5L_g + \Delta) \quad (45)$$

Equations can be written that will allow one to determine, rather easily, whether or not the chevron effect produces a beam moment larger than what would be calculated considering only the unbalanced vertical loads. It's important to recognize the local connection effects produce no beam end reactions. Thus, the beam end reactions R_1 and R_2 are a function of only the unbalanced vertical load (ΣV_i). By setting Equations 44 and 45 equal, one could calculate an equivalent gusset length, $L_{g,eq}$, that would produce the same beam moment change, ΔM , using either Equation 44 or 45. If the actual gusset length, L_g , is larger than $L_{g,eq}$, the beam moment using the symbiotic method will be smaller than what would be calculated using the connection designer's current method (i.e., if the connection designer even checked beam moment).

Setting Equations 44 and 45 equal, and setting L_g equal to $L_{g,eq}$,

$$\begin{aligned} \Delta M_{local} = 0.5w_l x^2 + (R_1 + q)x &= \Delta M_{unbal} = R_1(0.5L_g + \Delta) \\ 0.5w_l x^2 + (R_1 + q)x &= R_1(0.5L_{g,eq} + \Delta) \end{aligned} \quad (46)$$

Substituting Equation 28, which is in terms of x_1 , for x into Equation 46 and solving for $L_{g,eq}$ gives a quadratic equation. It's important to recognize that the terms w_l and q are also a function of L_g and that when Δ is nonzero, $q = [(M_{a-a})_T - (\Sigma V)_T \Delta] / L_g$.

When Δ is nonzero, the quadratic equation is the closed-form equation shown in Equation 47. In Equation 47, the square root of the discriminant, η , is given as a separate calculation for simplification. When using this equation, the negative value of the square root of the discriminant is used.

$$L_{g,eq} = \frac{M_T \left(\frac{b}{L} \right) - \eta}{(\Sigma V)_T \left[\frac{b}{L} - \left(\frac{b}{L} \right)^2 \right]} \quad (47a)$$

$$\eta = \sqrt{(\Sigma V)_T^2 \Delta^2 \left[\frac{b}{L} - \left(\frac{b}{L} \right)^2 \right] + (\Sigma V)_T M_T \Delta \left[-8 \left(\frac{b}{L} \right)^3 + 10 \left(\frac{b}{L} \right)^2 - 2 \left(\frac{b}{L} \right) \right] + M_T^2 \left(\frac{b}{L} \right)} \quad (47b)$$

In Equation 47, the term M_T is the total moment acting on the upper and lower gussets calculated using Equations 4 and 13 $[(M_{a-a})_l$ and $(M_{a-a})_b$, respectively].

When Δ is equal to zero, the quadratic shown in Equation 47 reduces to the closed-form equation shown in Equation 48:

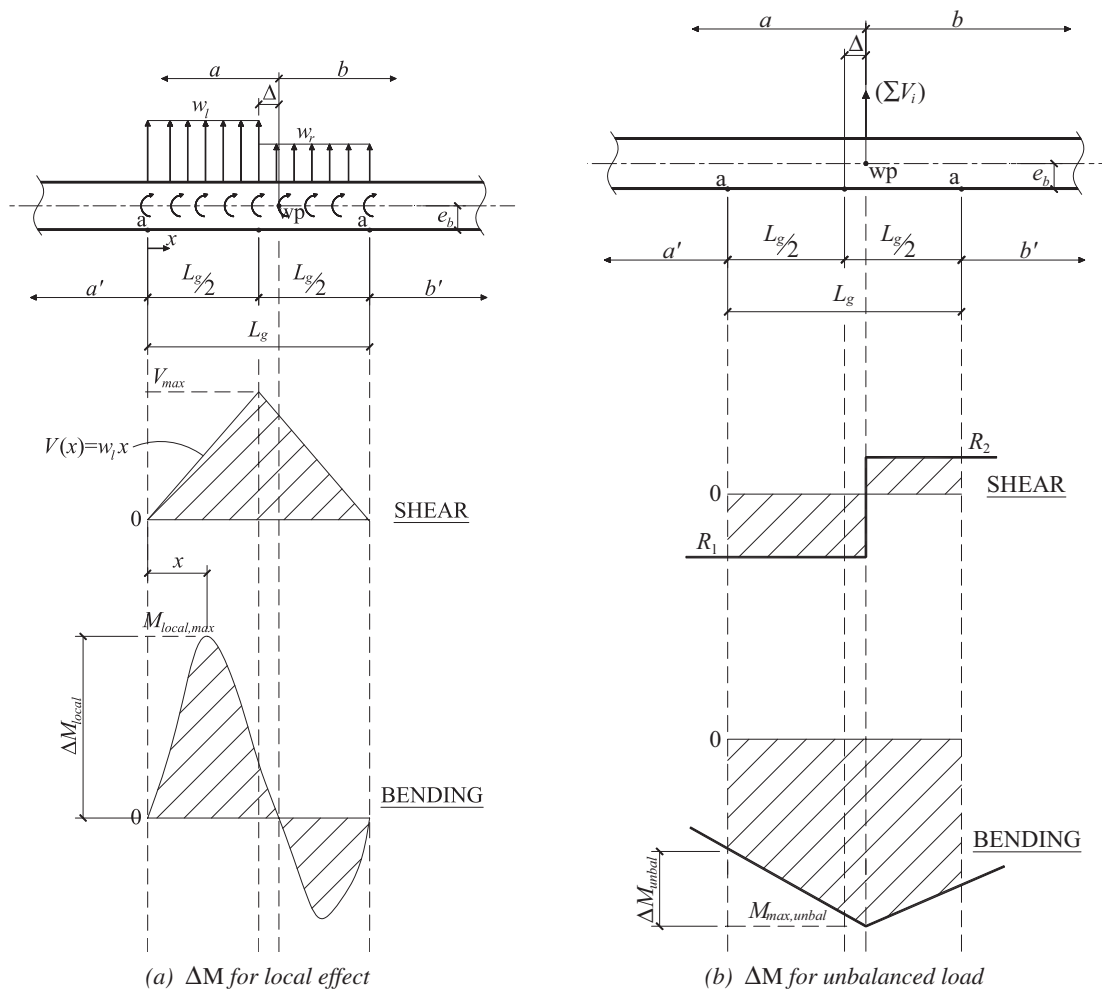


Fig. 6. Change in beam moment from edge of gusset to maximum moment.

$$L_{g,eq} = \frac{M_T}{(\Sigma V)_T} \left[\frac{\frac{b}{L} - \sqrt{\frac{b}{L}}}{\frac{b}{L} - \left(\frac{b}{L}\right)^2} \right] \quad (48)$$

- When L_g is smaller than $L_{g,eq}$, then an analysis that includes the chevron effect will result in a moment that is larger than the moment calculated neglecting the chevron effect (Pab/L is unconservative for bending).
- When L_g is larger than $L_{g,eq}$, then an analysis that includes the chevron effect will result in a moment that is smaller than the moment calculated neglecting the chevron effect (Pab/L is conservative for bending).

Comparison of Unbalanced Vertical Forces

The maximum beam moment using the symbiotic method given by Equation 26 can be set equal to the maximum moment calculated using the current beam designer's, which is Pab/L and is equal to the left beam end reaction, R_1 multiplied by the distance from the left beam end to the location of the work point, a (R_1a). By setting these two equations equal to each other, an equivalent unbalanced vertical force, $(\Sigma V)_T$, can be determined, thereby identifying a magnitude of unbalanced vertical force for which both equations will give the same maximum moment. Setting Equation 26 equal to R_1a gives

$$R_1a' + R_1x_1 + 0.5w_lx_1^2 + qx_1 = R_1a \quad (49)$$

The left beam end reaction, R_1 , in terms of the unbalanced vertical force, $(\Sigma V)_T$, is given by Equation 20. Equation 28 provides a relationship between x_1 and R_1 , and Equation 22 gives a relationship for w_l with the unbalanced vertical force, $(\Sigma V)_T$. The equation for w_l is also a function of the interface moments, $(M_{a-a})_l$ and $(M_{a-a})_b$. Given these relationships, some tedious substitutions, and taking $(\Sigma V)_T$ to be equal to an equivalent unbalanced vertical force for which both equations produce the same moment, $(\Sigma V)_{T,eq}$, gives the following equation:

$$(\Sigma V)_{T,eq} = \frac{q \left[\frac{b}{L} + \frac{4\Delta}{L_g} \left(\frac{b}{L} \right) \right] \pm q \sqrt{\left(\frac{b}{L} \right)^2 \left(\frac{8\Delta}{L_g} + \frac{16\Delta^2}{L_g^2} \right) + \left(\frac{b}{L} \right) \left(1 - \frac{2\Delta}{L_g} - \frac{8\Delta^2}{L_g^2} \right)}}{\left(\frac{b}{L} \right) \left(1 - \frac{2\Delta}{L_g} - \frac{8\Delta^2}{L_g^2} \right) - \left(\frac{b}{L} \right)^2} \quad (50)$$

Equation 50 reduces to a simpler form when the eccentricity, Δ , is equal to zero, as shown in Equation 51.

The roots of Equations 50 and 51 of interest for this application are the negative roots. Therefore, if the eccentricity, Δ , is non-zero, the equivalent unbalanced vertical force, $(\Sigma V)_{T,eq}$, is given by Equation 52:

$$(\Sigma V)_{T,eq} = q \left[\frac{\frac{b}{L} \pm \sqrt{\frac{b}{L}}}{\frac{b}{L} - \left(\frac{b}{L}\right)^2} \right] \quad (51)$$

$$(\Sigma V)_{T,eq} = \frac{q \left[\frac{b}{L} + \frac{4\Delta}{L_g} \left(\frac{b}{L} \right) \right] - q \sqrt{\left(\frac{b}{L} \right)^2 \left(\frac{8\Delta}{L_g} + \frac{16\Delta^2}{L_g^2} \right) + \left(\frac{b}{L} \right) \left(1 - \frac{2\Delta}{L_g} - \frac{8\Delta^2}{L_g^2} \right)}}{\left(\frac{b}{L} \right) \left(1 - \frac{2\Delta}{L_g} - \frac{8\Delta^2}{L_g^2} \right) - \left(\frac{b}{L} \right)^2} \quad (52)$$

If the eccentricity, Δ , is zero, the equivalent unbalanced vertical force, $(\Sigma V)_{T,eq}$, is given by Equation 53:

$$(\Sigma V)_{T,eq} = q \left[\frac{\frac{b}{L} - \sqrt{\frac{b}{L}}}{\frac{b}{L} - \left(\frac{b}{L}\right)^2} \right] \quad (53)$$

A few comments regarding the use of Equations 52 and 53:

- The signs of the quantities $(\Sigma V)_{T,eq}$ and $(\Sigma V)_T$ will be the same. For example, if the actual total unbalanced vertical force, $(\Sigma V)_T$, is negative, the quantity calculated from Equation 52 (or 53), $(\Sigma V)_{T,eq}$, will also be negative, and vice versa.
- When the absolute value of $(\Sigma V)_{T,eq}$ is smaller than the absolute value of $(\Sigma V)_T$, then an analysis that includes the chevron effect will result in a moment that is smaller than the moment calculated neglecting the chevron effect (Pab/L is conservative for bending).
- When the absolute value of $(\Sigma V)_{T,eq}$ is larger than the absolute value of $(\Sigma V)_T$, then an analysis that includes the chevron effect will result in a moment that is larger than the moment calculated neglecting the chevron effect (Pab/L is unconservative for bending).

Note that every term in Equations 52 and 53 is a function of the position of the work point along the span of the beam, b/L . Although it may be counterintuitive to some, Equations 52 and 53 show that the position of the work point along the span of the beam has an effect on whether or not the chevron effect will dominate maximum beam moment.

Possible Beam Shear Diagrams

Unlike beam moment, the local effects of the connection will almost always give a beam shear in excess of the beam shear determined by assuming the unbalanced vertical load acts as a concentrated load at the work point. Figure 7a shows a representative beam shear diagram of this case. However, there are rare instances when the net transverse loads on the beam, w_l and w_r , act in the same direction. This occurs when the magnitude of the uniformly distributed plastic moment acting on section a-a (see Figure 1) is smaller than the magnitude of the net uniformly distributed unbalanced vertical load. In this case, the maximum beam shear calculated using the symbiotic method will be equal to the beam end reaction. Figure 7b shows a representative beam shear diagram for this case.

Note that it is assumed that the unbalanced vertical load acts downward for the shear diagrams shown in Figure 7. When the unbalanced vertical force acts upward, the beam shear diagrams would be mirrored about the x -axis to those shown in Figure 7.

Possible Beam Moment Diagrams

Many factors affect the beam moment diagram in a chevron frame; relative magnitude of the unbalanced vertical force, the direction of the unbalanced vertical force (up or down), the magnitude of the tension brace force relative to the compression brace force, whether or not the tension brace is on the left side and the compression brace on the right side or vice versa can all affect the beam shear diagram. Figure 8 shows some possible diagrams.

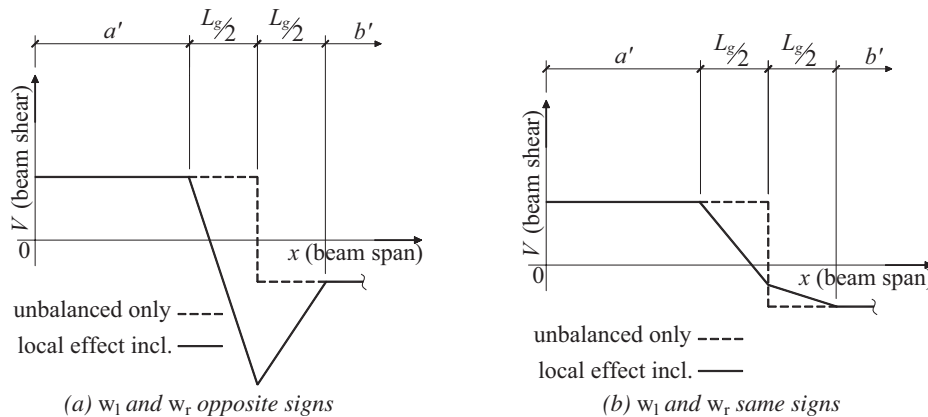


Fig. 7. Representative beam shear diagrams.

In the diagrams shown in Figure 8, it is assumed that the unbalanced vertical force acts downward. Readers should be aware that this is not always the case—for example, if the braces frame to only the bottom side of the beam and the magnitude of the compression brace is larger than that of the tension brace, the unbalanced vertical force will act upward resulting in moment diagrams that would be mirrored about the x -axis to those diagrams shown in Figure 8.

When the unbalanced vertical force is zero (a balanced case) or relatively small, the chevron effect will dominate the demands on the beam relative to considering only the unbalanced vertical load (i.e., the current beam designer method). Figure 8a shows a representative moment diagram for such a case. The required beam moment calculated neglecting the local effect of the connection can be significantly underestimated when the unbalanced load is relatively small.

When q and R_1 are the same sign, the maximum moment calculated considering the local effect will be maximum within the left half of the gusset, but whether the local effect is dominant depends on the relative magnitude of the unbalanced load. See Figures 8a and 8b.

When q and R_1 have different signs, one of two things will occur: (1) The local effect does not dominate the maximum moment (see Figure 8c), and considering the local effects will result in a lighter beam in regard to required moment, or (2) the maximum moment considering the local effects occurs within the right half of the gusset (see Figure 8d), but whether the local effect is dominant varies on the relative magnitude of the unbalanced load. In this case, the maximum moment should be evaluated using the equations derived above for $M(x_2)$.

Additionally, the moment diagram shown in Figure 8d shows a case where the local effect is dominant. This type of diagram occurs when q and R_1 have different signs and $M_{max,local}$ is less than $M_{max,unbal}$. Equations for calculating $M_{max,local}$ and $M_{max,unbal}$ were derived in the “Evaluating the Chevron Effect” section.

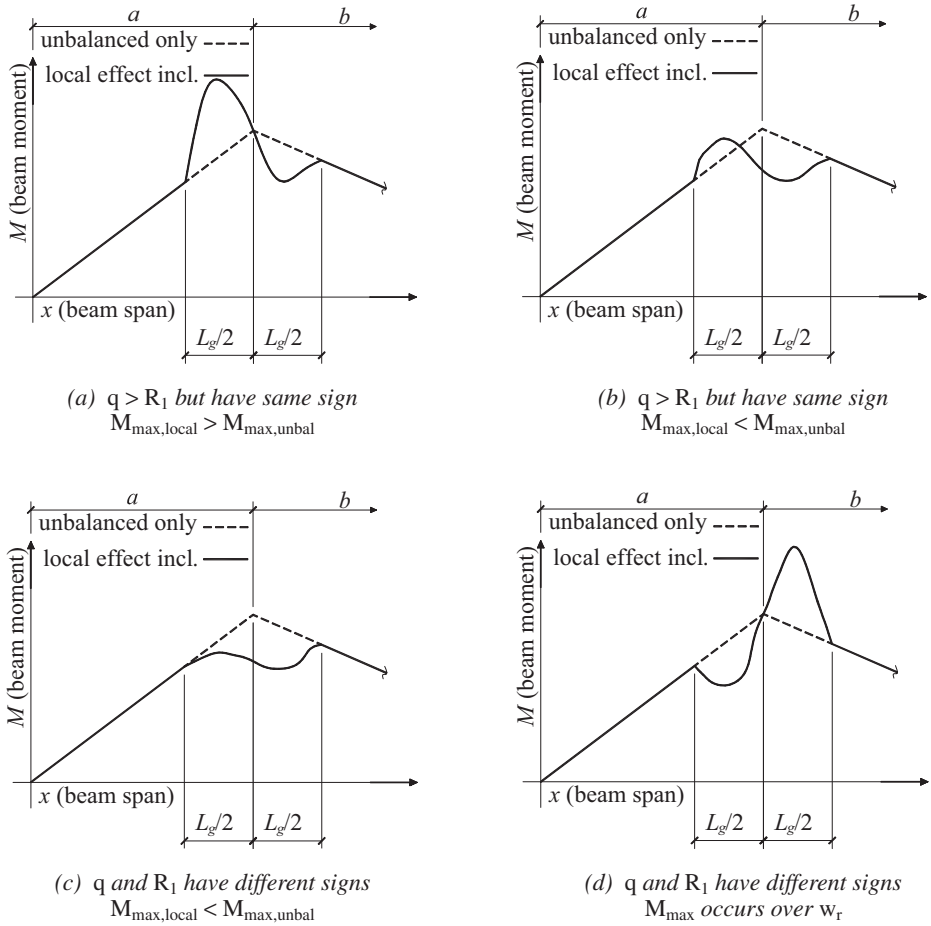


Fig. 8. Representative beam moment diagrams. (Note: Δ is assumed to be zero in these figures.)

EXAMPLE PROBLEM 1

The braced frame shown in the elevation in Figure 9a is used in a special concentrically braced frame. Figure 9b shows the brace forces calculated using the requirements of Section F2.3 of AISC 341-16 (AISC, 2016), which requires an analysis of the frame when the compression braces reach their expected buckling and post-buckling strength while the tension brace reaches its expected tension strength.

Part 1

Considering only the brace forces and load cases shown in Figure 9b for joint 1,

- Determine the approximate gusset length, $L_{g,approx}$, and half-beam depth, $e_{b,app}$.
- Use the proposed equations, using the approximate gusset geometry,
 - To determine if the chevron effect needs to be considered for the required beam moment.
 - To size the beam for shear and bending. Check both load cases; buckling load case and post-buckling load case.

Note that beam selected in this part will be the beam used by the connection designer for performing Part 2 of the problem. Additionally, the beam designer does not communicate the approximated gusset length, $L_{g,app}$, determined in this part to the connection designer for the work to be performed Part 2.

Part 2

Figure 10 shows the connection geometry (chosen by the connection designer) and brace forces for the two load cases being considered. Note that this is not necessarily the L_g dimension approximated by the beam designer in Part 1. The beam size given in Figure 10 is the beam size provided by the beam designer as given in Part 1 of this problem.

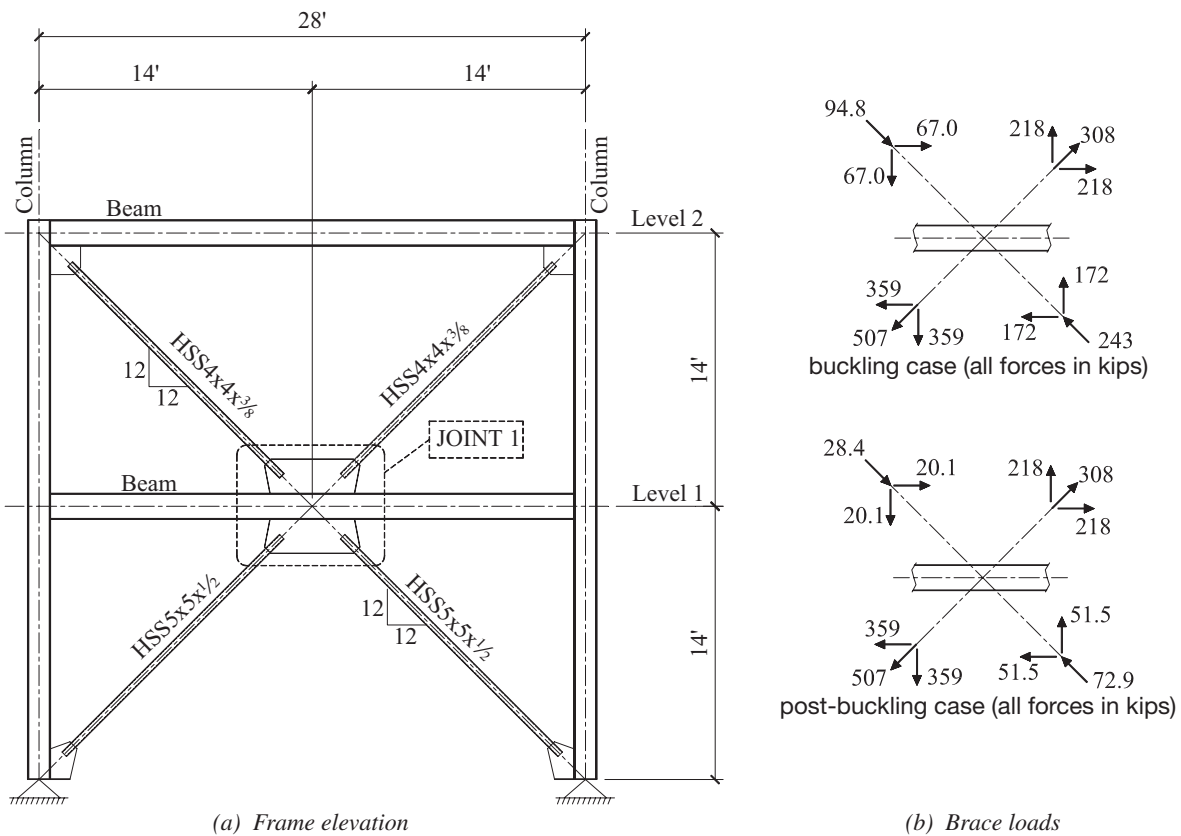


Fig. 9. Braced frame elevation and brace loads.

- Draw free-body diagrams of the left and right halves of the gussets showing the forces acting on sections a-a and b-b for both the top and bottom gussets (similar to Figure 1).
- Draw beam-loading diagrams for the two load cases showing the uniformly distributed loads and moments acting on the beam due to the brace forces (similar to Figure 4).

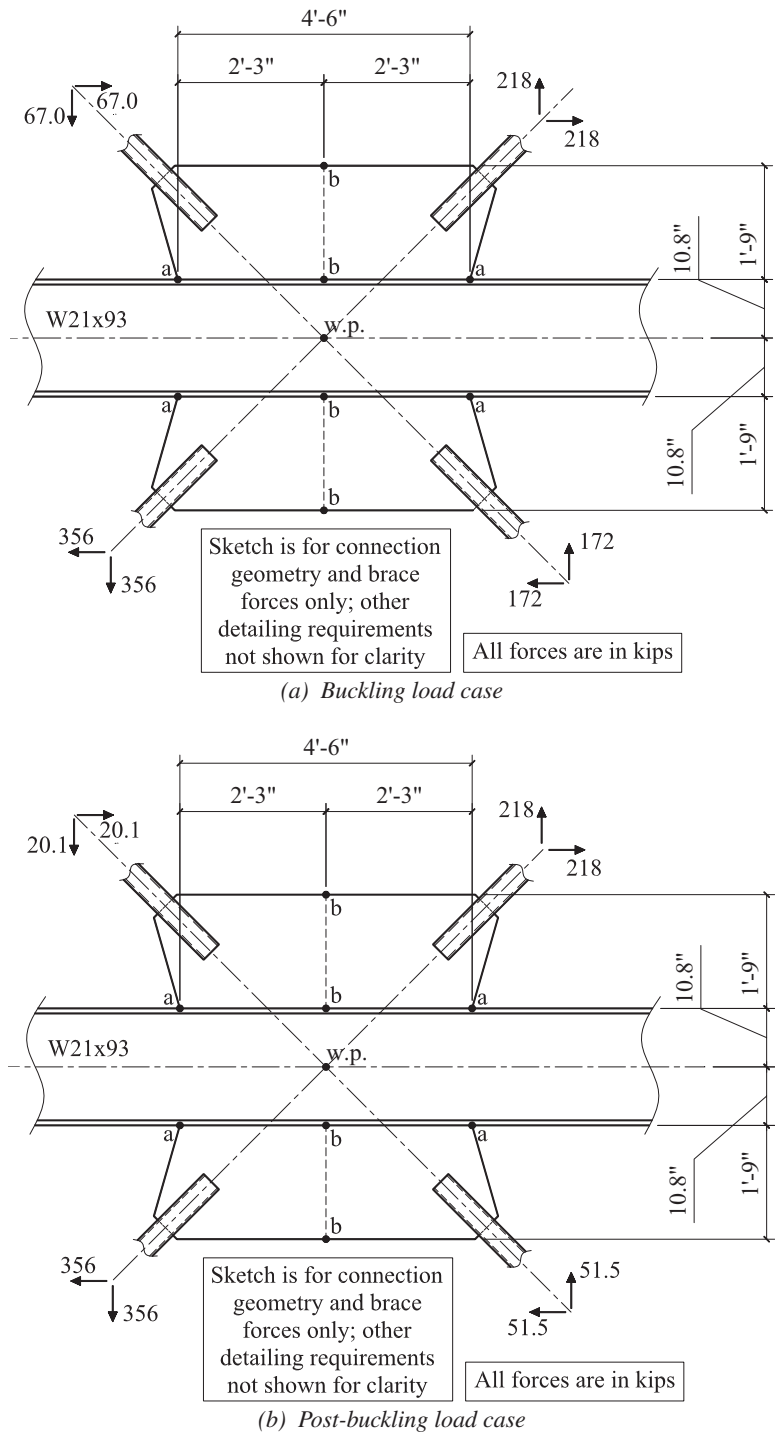


Fig. 10. Connection geometry and brace forces.

Part 3

Draw the beam shear and moment diagrams for both load cases. On each diagram, show plots for the two paradoxical methods (current standard of care used by beam designers and connection designers) as well as the symbiotic method.

Solution

General Calculations

Buckling load case:

$$\begin{aligned}(\Sigma V)_t &= (-67.0 \text{ kips}) + 218 \text{ kips} \\ &= 151 \text{ kips}\end{aligned}$$

$$\begin{aligned}(\Sigma V)_b &= (-359 \text{ kips}) + 172 \text{ kips} \\ &= -187 \text{ kips}\end{aligned}$$

$$\begin{aligned}(\Sigma H)_t &= (67.0 \text{ kips}) + 218 \text{ kips} \\ &= 285 \text{ kips}\end{aligned}$$

$$\begin{aligned}(\Sigma H)_b &= (-359 \text{ kips}) + (-172 \text{ kips}) \\ &= -531 \text{ kips}\end{aligned}$$

$$\begin{aligned}(\Sigma V)_T &= (151 \text{ kips}) + (-187 \text{ kips}) \\ &= -36.0 \text{ kips}\end{aligned}$$

Similar to Equation 21, the total net horizontal load, $(\Sigma H)_T$ is

$$\begin{aligned}(\Sigma H)_T &= (\Sigma H)_t + (\Sigma H)_b \\ &= 285 \text{ kips} + (-531 \text{ kips}) \\ &= -246 \text{ kips}\end{aligned}$$

Post-buckling load case:

$$\begin{aligned}(\Sigma V)_t &= (-20.1 \text{ kips}) + 218 \text{ kips} \\ &= 197.9 \text{ kips}\end{aligned}$$

$$\begin{aligned}(\Sigma V)_b &= (-359 \text{ kips}) + 51.5 \text{ kips} \\ &= -307.5 \text{ kips}\end{aligned}$$

$$\begin{aligned}(\Sigma H)_t &= 20.1 \text{ kips} + 218 \text{ kips} \\ &= 238.1 \text{ kips}\end{aligned}$$

$$\begin{aligned}(\Sigma H)_b &= (-359 \text{ kips}) + (-51.1 \text{ kips}) \\ &= -410.5 \text{ kips}\end{aligned}$$

$$\begin{aligned}(\Sigma V)_T &= 197.9 \text{ kips} + (-307.5 \text{ kips}) \\ &= -109.6 \text{ kips}\end{aligned}$$

$$\begin{aligned}(\Sigma H)_T &= 238.1 \text{ kips} + (-410.5 \text{ kips}) \\ &= -172.4 \text{ kips}\end{aligned}$$

Part 1

The approximate length of the gusset, $L_{g,app}$, and half-depth of the beam, $e_{b,app}$ (Fortney and Thornton, 2015) can be determined using Equations 42 and 43, respectively:

$$\begin{aligned} L_{g,app} &= \frac{L}{6} \\ &= \frac{(28 \text{ ft})(12 \text{ in./ft})}{6} \\ &= 56.0 \text{ in.} \end{aligned} \quad (42)$$

$$\begin{aligned} e_{b,app} &= (0.375)(\text{span of beam in feet}) \\ &= (0.375)(28 \text{ ft}) \\ &= 10.5 \text{ in.} \end{aligned} \quad (43)$$

Equation 48 ($\Delta = 0$) can be used to determine if the chevron effect needs to be considered in regard to beam bending. Equation 48 requires the calculation of M_T [Equations 4 and 13, for $(M_{a-a})_b$ and $(M_{a-a})_t$, respectively].

Buckling Load Case

The gusset interface moments for the buckling case are (noting that $\Delta = 0$ for this problem)

$$\begin{aligned} (M_{a-a})_t &= (H_1 + H_2)_t e_b + (V_1 + V_2)_t \Delta \\ &= (67.0 \text{ kips} + 218 \text{ kips})(10.5 \text{ in.}) + [(-67.0 \text{ kips}) + 218 \text{ kips}](0 \text{ in.}) \\ &= 2,993 \text{ kip-in.} \end{aligned} \quad (13)$$

$$\begin{aligned} (M_{a-a})_b &= (V_1 + V_2)_b \Delta - (H_1 + H_2)_b e_b \\ &= (-359 \text{ kips} + 172 \text{ kips})(0 \text{ in.}) - [(-359 \text{ kips}) + -172 \text{ kips}](10.5 \text{ in.}) \\ &= 5,576 \text{ kip-in.} \end{aligned} \quad (4)$$

$$\begin{aligned} M_T &= (M_{a-a})_t + (M_{a-a})_b \\ &= 2,993 \text{ kips-in.} + 5,576 \text{ kips-in.} \\ &= 8,569 \text{ kip-in.} \end{aligned}$$

The net uniformly distributed moment, q , is

$$\begin{aligned} q &= \left[(\Sigma H)_t - (\Sigma H)_b \right] \left(\frac{e_b}{L_g} \right) \\ &= [285 \text{ kips} - (-531 \text{ kips})] \left(\frac{10.5 \text{ in.}}{56.0 \text{ in.}} \right) \\ &= 153 \text{ kip-in./in.} \end{aligned} \quad (25)$$

The net uniformly distributed load on the left half of the gusset, w_l , is

$$\begin{aligned} w_l &= - \left(\frac{4M_{a-a}}{L_g^2} \right)_t - \left(\frac{4M_{a-a}}{L_g^2} \right)_b + \left(\frac{\Sigma V}{L_g} \right)_t + \left(\frac{\Sigma V}{L_g} \right)_b \\ &= - \left[\frac{(4)(2,993 \text{ kip-in.})}{(56.0 \text{ in.})^2} \right] - \left[\frac{(4)(5,576 \text{ kip-in.})}{(56.0 \text{ in.})^2} \right] + \left(\frac{151 \text{ kips}}{56.0 \text{ in.}} \right) + \left(\frac{-187 \text{ kips}}{56.0 \text{ in.}} \right) \\ &= -11.6 \text{ kip/in.} \end{aligned} \quad (22)$$

The left beam end reaction, R_1 , is

$$\begin{aligned}
 R_1 &= \frac{-(\Sigma V)_T b}{L} \\
 &= \frac{-(-36.0 \text{ kips})(14 \text{ ft})}{28 \text{ ft}} \\
 &= 18.0 \text{ kips}
 \end{aligned} \tag{20}$$

The equivalent gusset length, $L_{g,eq}$ is

$$\begin{aligned}
 L_{g,eq} &= \frac{M_T}{(\Sigma V)_T} \left[\frac{\frac{b}{L} - \sqrt{\frac{b}{L}}}{\frac{b}{L} - \left(\frac{b}{L}\right)^2} \right] \\
 &= \frac{8,569 \text{ kip-in.}}{-36.0 \text{ kips}} \left[\frac{\left(\frac{14 \text{ ft}}{28 \text{ ft}}\right) - \sqrt{\frac{14 \text{ ft}}{28 \text{ ft}}}}{\left(\frac{14 \text{ ft}}{28 \text{ ft}}\right) - \left(\frac{14 \text{ ft}}{28 \text{ ft}}\right)^2} \right] \\
 &= 197 \text{ in.} > L_{g,app} = 56.0 \text{ in.}
 \end{aligned} \tag{48}$$

The chevron effect will dominate the beam moment, producing a larger moment relative to the classical Pab/L type of analysis (i.e., the beam designer's approach). It is unreasonable to consider increasing the gusset length to 135 in.

Post-Buckling Load Case

The gusset interface moments for the post-buckling case are

$$\begin{aligned}
 (M_{a-a})_t &= (H_1 + H_2)_t e_b + (V_1 + V_2)_t \Delta \\
 &= (20.1 \text{ kips} + 218 \text{ kips})(10.5 \text{ in.}) + [(-20.1 \text{ kips}) + 218 \text{ kips}](0 \text{ in.}) \\
 &= 2,500 \text{ kip-in.}
 \end{aligned} \tag{13}$$

$$\begin{aligned}
 (M_{a-a})_b &= (V_1 + V_2)_b \Delta - (H_1 + H_2)_b e_b \\
 &= (-359 \text{ kips} + 51.5 \text{ kips})(0 \text{ in.}) - [-359 \text{ kips} + (-51.5 \text{ kips})](10.5 \text{ in.}) \\
 &= 4,310 \text{ kip-in.}
 \end{aligned} \tag{4}$$

The net uniformly distributed moment, q , is

$$\begin{aligned}
 q &= \left[(\Sigma H)_t - (\Sigma H)_b \right] \left(\frac{e_b}{L_g} \right) \\
 &= [238.1 \text{ kips} - (-410.5 \text{ kips})] \left(\frac{10.5 \text{ in.}}{56.0 \text{ in.}} \right) \\
 &= 122 \text{ kip-in./in.}
 \end{aligned} \tag{25}$$

The net uniformly distributed load on the left half of the gusset, w_l , is

$$\begin{aligned}
 w_l &= - \left(\frac{4M_{a-a}}{L_g^2} \right)_t - \left(\frac{4M_{a-a}}{L_g^2} \right)_b + \left(\frac{\Sigma V}{L_g} \right)_t + \left(\frac{\Sigma V}{L_g} \right)_b \\
 &= - \left(\frac{4(2,500 \text{ kip-in.})}{(56.0 \text{ in.})^2} \right) - \left(\frac{4(4,310 \text{ kip-in.})}{(56.0 \text{ in.})^2} \right) + \left(\frac{197.9 \text{ kips}}{56.0 \text{ in.}} \right) + \left(\frac{-307.5 \text{ kips}}{56.0 \text{ in.}} \right) \\
 &= -10.7 \text{ kip/in.}
 \end{aligned} \tag{22}$$

The left beam end reaction, R_1 , is

$$\begin{aligned}
 R_1 &= \frac{-(\Sigma V)_T b}{L} \\
 &= \frac{-(-109.6 \text{ kips})(14 \text{ ft})}{28 \text{ ft}} \\
 &= 54.8 \text{ kips}
 \end{aligned} \tag{20}$$

The equivalent gusset length, $L_{g,eq}$ is

$$\begin{aligned}
 L_{g,eq} &= \frac{M_T}{(\Sigma V)_T} \left[\frac{\frac{b}{L} - \sqrt{\frac{b}{L}}}{\frac{b}{L} - \left(\frac{b}{L}\right)^2} \right] \\
 &= \frac{6,810 \text{ kip-in.}}{-109.6 \text{ kips}} \left[\frac{0.50 - \sqrt{0.50}}{0.50 - (0.50)^2} \right] \\
 &= 51.5 \text{ in.} < L_{g,app} = 56.0 \text{ in.}
 \end{aligned} \tag{48}$$

The chevron effect will not dominate the beam moment and will produce a slightly smaller moment relative to the classical Pab/L type of analysis.

The maximum beam shear can be calculated using Equation 33.

For the buckling case, $R_1 = 18.0$ kips, $w_l = -11.6$ kip/in., and V_{max} is then

$$\begin{aligned}
 V_{max} &= R_1 + 0.5w_l L_g \\
 &= 18.0 \text{ kips} + 0.5(-11.6 \text{ kip-in.})(56.0 \text{ in.}) \\
 &= -307 \text{ kips}
 \end{aligned} \tag{33}$$

For the post-buckling case, $R_1 = 54.8$ kips, $w_l = -10.7$ kip/in., and V_{max} is then

$$\begin{aligned}
 V_{max} &= 54.8 \text{ kips} + 0.5(-10.7 \text{ kip-in.})(56.0 \text{ in.}) \\
 &= -245 \text{ kips}
 \end{aligned}$$

For both load cases, w_l acts downward. As discussed previously, w_l is the second derivative of $M(x_1)$; when w_l acts downward, the maximum moment occurs along the left half of the gusset. Therefore, Equation 30 can be used to calculate the maximum beam moment, using Equation 28 to determine the location of maximum moment (x_1).

The maximum beam moment for the buckling case is located at

$$\begin{aligned}
 x_1 &= \frac{-R_1 - q}{w_l} \\
 &= \frac{-18.0 \text{ kips} - 153 \text{ kip-in./in.}}{-11.6 \text{ kip/in.}} \\
 &= 14.8 \text{ in.}
 \end{aligned} \tag{28}$$

and is

$$\begin{aligned}
 M_{max} &= R_1 a' + (R_1 + q) \left(\frac{-R_1 - q}{w_l} \right) + 0.5w_l \left(\frac{-R_1 - q}{w_l} \right)^2 \\
 &= (18.0 \text{ kips})(14.0 \text{ in.}) + (18.0 \text{ kips} + 153 \text{ kips})(14.8 \text{ in.}) + 0.5(-11.6 \text{ kip/in.})(14.8 \text{ in.})^2 \\
 &= 3,780 \text{ kip-in.}
 \end{aligned} \tag{30}$$

Table 1. Maximum Beam Shear and Moment		
Load Case	V_{max}	M_{max}
	(kips)	(kip-in.)
Buckling	-307	3780
Post-buckling	-245	9130

The maximum beam moment for the post-buckling case is located at

$$x_1 = \frac{-54.8 \text{ kips} - 122 \text{ kip-in./in.}}{-10.7 \text{ kip/in.}}$$

$$= 16.5 \text{ in.}$$

and is

$$M_{max} = (54.8 \text{ kips})(140 \text{ in.}) + (54.8 \text{ kips} + 122 \text{ kips})(16.5 \text{ in.}) + 0.5(-10.7 \text{ kip/in.})(16.5 \text{ in.})^2$$

$$= 9,130 \text{ kip-in.}$$

As can be seen in Table 1, the buckling case gives the largest beam shear, -307 kips, and the post-buckling case gives the largest beam moment, 9,130 kip-in. A beam size will be selected for these values. Also recall that the beam half-depth, e_b , was approximated to be 10.5 in. Therefore, a beam size will be selected from the W21 family.

Assuming the beam will be laterally braced such that its plastic bending strength can be reached, the required plastic section modulus, Z_{req} , is

$$Z_{req} = \frac{9,130 \text{ kip-in.}}{(0.9)(50 \text{ ksi})}$$

$$= 203 \text{ in.}^3$$

Using AISC *Manual* Table 3-2 (AISC, 2017), a W21×93 has an available design shear and flexural strength of 376 kips and 9,948 kip-in., respectively.

Final beam size: W21×93

Part 2

The force distributions in the top and bottom connections for the buckling and post-buckling load cases are shown in Figures 11a and 11b, respectively. The force distribution equations given in Equations 2 through 19 were used to calculate the forces and moment shown, but the calculations are not shown here in order to conserve space. Fortney and Thornton (2015) provide several examples showing the use of these equations.

Beam Loading Using the Symbiotic Method

Buckling load case:

The moments, $(M_{a-a})_t$ and $(M_{a-a})_b$, are

$$(M_{a-a})_t = (H_1 + H_2)_t e_b + (V_1 + V_2)_t \Delta \tag{13}$$

$$(M_{a-a})_t = (67.0 \text{ kips} + 218 \text{ kips})(10.8 \text{ in.}) + (-67.0 \text{ kips} + 218 \text{ kips})(0 \text{ in.})$$

$$= 3,078 \text{ kip-in.}$$

$$(M_{a-a})_b = (V_1 + V_2)_b \Delta - (H_1 + H_2)_b e_b \quad (4)$$

$$\begin{aligned} (M_{a-a})_b &= (-359 \text{ kips} + 172 \text{ kips})(0 \text{ in.}) - [-359 \text{ kips} + (-172 \text{ kips})](10.8 \text{ in.}) \\ &= 5,735 \text{ kip-in.} \end{aligned}$$

$$\begin{aligned} M_T &= (M_{a-a})_t + (M_{a-a})_b \\ &= 3,078 \text{ kips-in.} + 5,735 \text{ kips-in.} \\ &= 8,813 \text{ kip-in.} \end{aligned}$$

The net uniformly distributed loads, w_l and w_r , can be calculated using Equations 22 and 23, respectively:

$$\begin{aligned} w_l &= -\left(\frac{4M_{a-a}}{L_g^2}\right)_t - \left(\frac{4M_{a-a}}{L_g^2}\right)_b + \left(\frac{\sum V}{L_g}\right)_t + \left(\frac{\sum V}{L_g}\right)_b \quad (22) \\ &= -\left(\frac{4(3,078 \text{ kip-in.})}{(54.0 \text{ in.})^2}\right) - \left(\frac{4(5,735 \text{ kip-in.})}{(54.0 \text{ in.})^2}\right) + \left(\frac{151 \text{ kips}}{54.0 \text{ in.}}\right) + \left(\frac{-187 \text{ kips}}{54.0 \text{ in.}}\right) \\ &= -12.8 \text{ kip/in.} \end{aligned}$$

$$\begin{aligned} w_r &= \left(\frac{4M_{a-a}}{L_g^2}\right)_t + \left(\frac{4M_{a-a}}{L_g^2}\right)_b + \left(\frac{\sum V}{L_g}\right)_t + \left(\frac{\sum V}{L_g}\right)_b \quad (23) \\ &= \left[\frac{4(3,078 \text{ kip-in.})}{(54.0 \text{ in.})^2}\right] + \left[\frac{4(5,735 \text{ kip-in.})}{(54.0 \text{ in.})^2}\right] + \left(\frac{151 \text{ kips}}{54.0 \text{ in.}}\right) + \left(\frac{-187 \text{ kips}}{54.0 \text{ in.}}\right) \\ &= 11.4 \text{ kip/in.} \end{aligned}$$

The net uniformly distributed moment, q , is

$$\begin{aligned} q &= [(\sum H)_t - (\sum H)_b] \left(\frac{e_b}{L_g}\right) \quad (25) \\ &= [285 \text{ kips} - (-531 \text{ kips})] \left(\frac{10.8 \text{ in.}}{54.0 \text{ in.}}\right) \\ &= 163 \text{ kip-in./in.} \end{aligned}$$

Given that $R_1 = 18.0$ kips (calculated previously), and the gusset length, L_g , is 54.0 in., the equivalent gusset length, $L_{g,eq}$, is

$$\begin{aligned} L_{g,eq} &= \frac{M_T}{(\sum V)_T} \left[\frac{\frac{b}{L} - \sqrt{\frac{b}{L}}}{\frac{b}{L} - \left(\frac{b}{L}\right)^2} \right] \quad (48) \\ &= \frac{8,813 \text{ kip-in.}}{-36.0 \text{ kips}} \left[\frac{0.50 - \sqrt{0.50}}{0.50 - (0.50)^2} \right] \\ &= 203 \text{ in.} > L_g = 54.0 \text{ in.} \end{aligned}$$

Therefore, the local effects will dominate the moment. However, for this example, the post-buckling case governs for beam moment.

Post-buckling load case:

The moments, $(M_{a-a})_t$ and $(M_{a-a})_b$, are

$$(M_{a-a})_t = (20.1 \text{ kips} + 218 \text{ kips})(10.8 \text{ in.}) + (-20.1 \text{ kips} + 218 \text{ kips})(0 \text{ in.}) = 2,571 \text{ kip-in.}$$

$$(M_{a-a})_b = (-359 \text{ kips} + 51.5 \text{ kips})(0 \text{ in.}) - [-359 \text{ kips} + (-51.5 \text{ kips})](10.8 \text{ in.}) = 4,433 \text{ kip-in.}$$

$$M_T = (M_{a-a})_t + (M_{a-a})_b = 2,571 \text{ kips-in.} + 4,433 \text{ kips-in.} = 7,004 \text{ kip-in.}$$

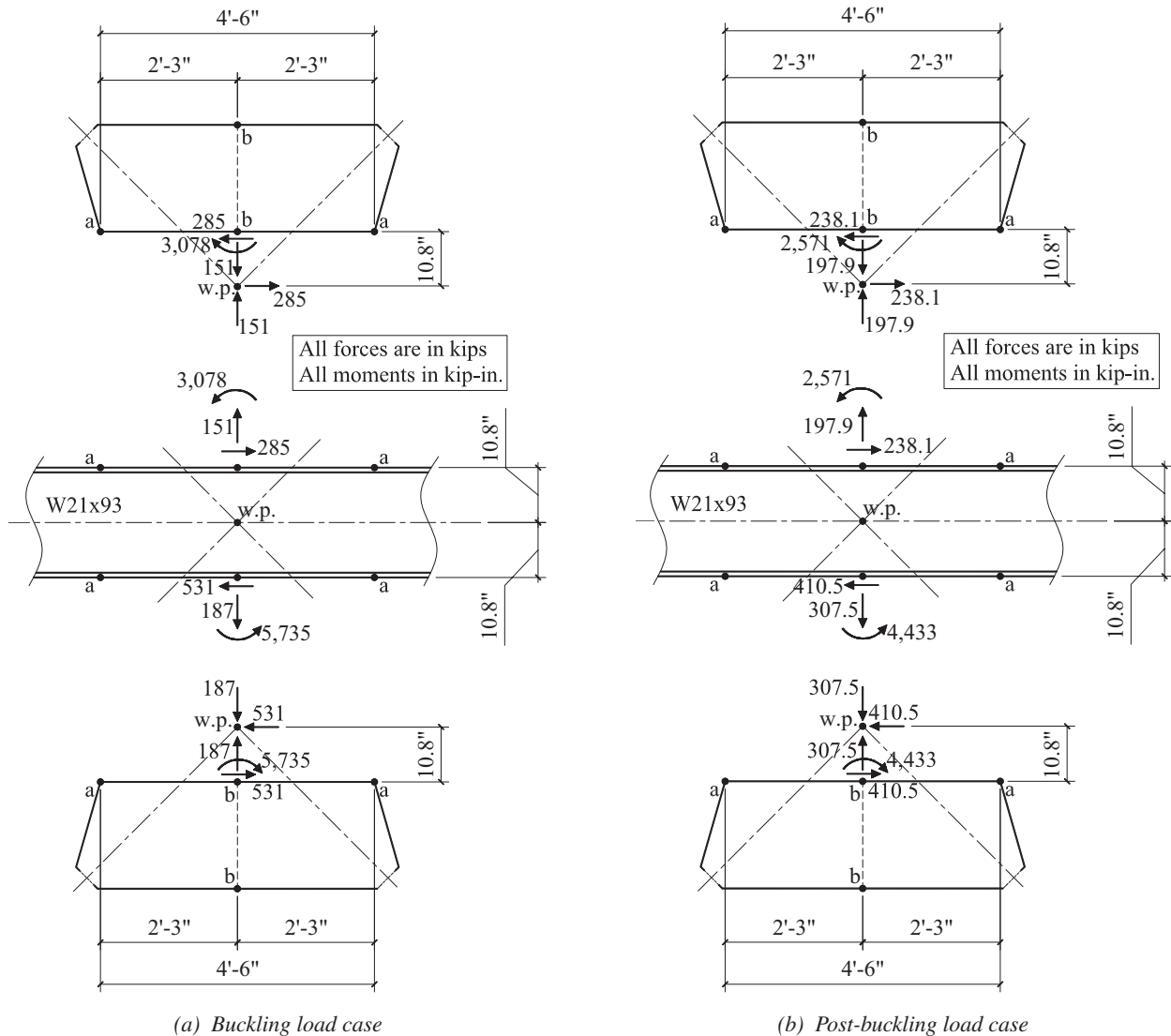


Fig. 11. Connection force distributions.

The net uniformly distributed loads, w_l and w_r , can be calculated using Equations 22 and 23, respectively:

$$w_l = -\left[\frac{4(2,571 \text{ kip-in.})}{(54.0 \text{ in.})^2} \right] - \left[\frac{4(4,433 \text{ kip-in.})}{(54.0 \text{ in.})^2} \right] + \left(\frac{197.9 \text{ kips}}{54.0 \text{ in.}} \right) + \left(\frac{-307.5 \text{ kips}}{54.0 \text{ in.}} \right)$$

$$= -11.6 \text{ kip/in.}$$

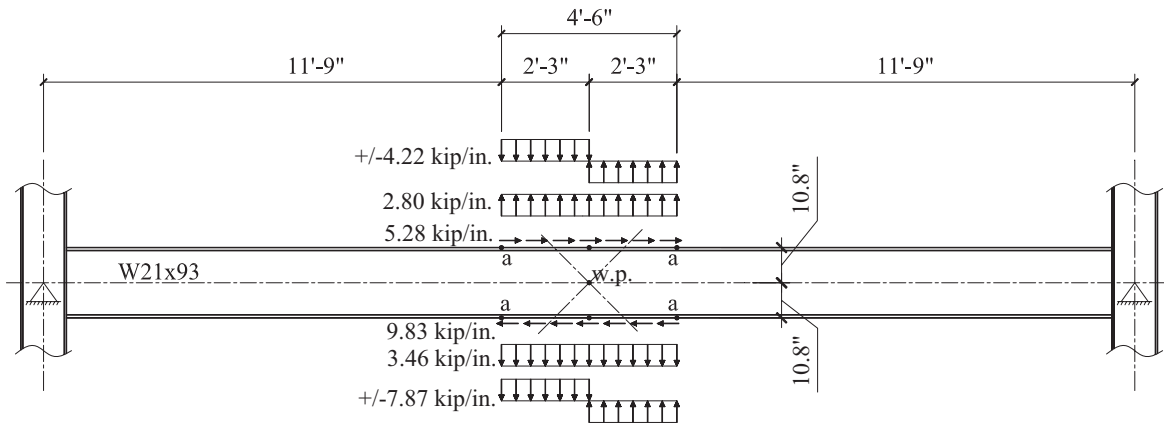
$$w_r = \left[\frac{4(2,571 \text{ kip-in.})}{(54.0 \text{ in.})^2} \right] + \left[\frac{4(4,433 \text{ kip-in.})}{(54.0 \text{ in.})^2} \right] + \left(\frac{197.9 \text{ kips}}{54.0 \text{ in.}} \right) + \left(\frac{-307.5 \text{ kips}}{54.0 \text{ in.}} \right)$$

$$= 7.58 \text{ kip/in.}$$

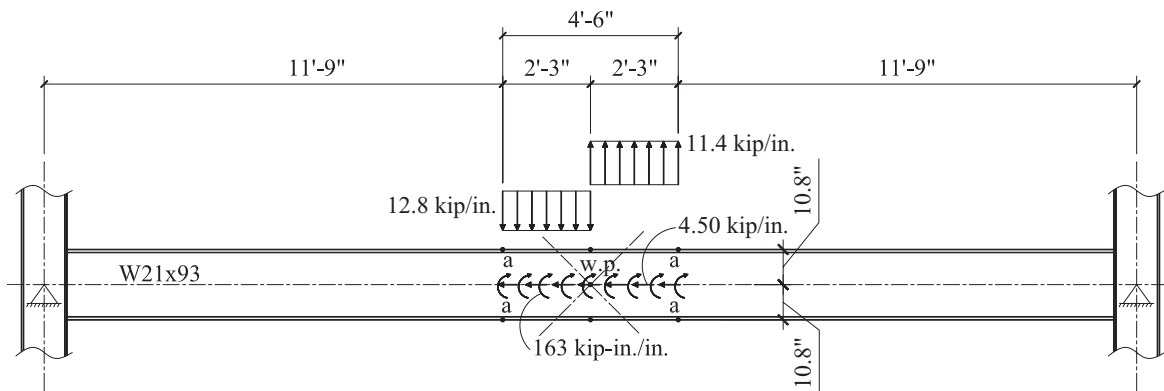
The net uniformly distributed moment, q , is

$$q = [238.1 \text{ kips} - (-410.5 \text{ kips})] \left(\frac{10.8 \text{ in.}}{54.0 \text{ in.}} \right)$$

$$= 130 \text{ kip-in./in.}$$



(a) Uniformly distributed beam loading



(b) Statically equivalent net beam loading

Fig. 12. Beam loading for buckling load case—sybiotic method.

Given that $R_1 = 54.8$ kips (calculated previously), and the gusset length, L_g , is 54.0 in., the equivalent gusset length, $L_{g,eq}$, is

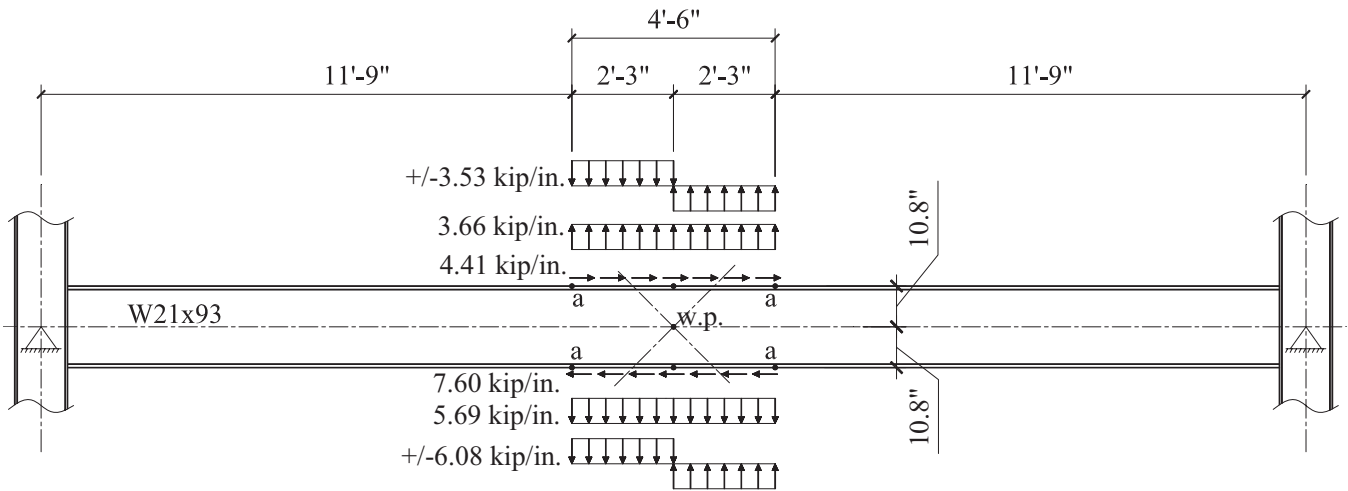
$$L_{g,eq} = \frac{7,004 \text{ kip-in.}}{-109.6 \text{ kips}} \left[\frac{0.50 - \sqrt{0.50}}{0.50 - (0.50)^2} \right]$$

$$= 52.9 \text{ in.} < L_g = 54.0 \text{ in.}$$

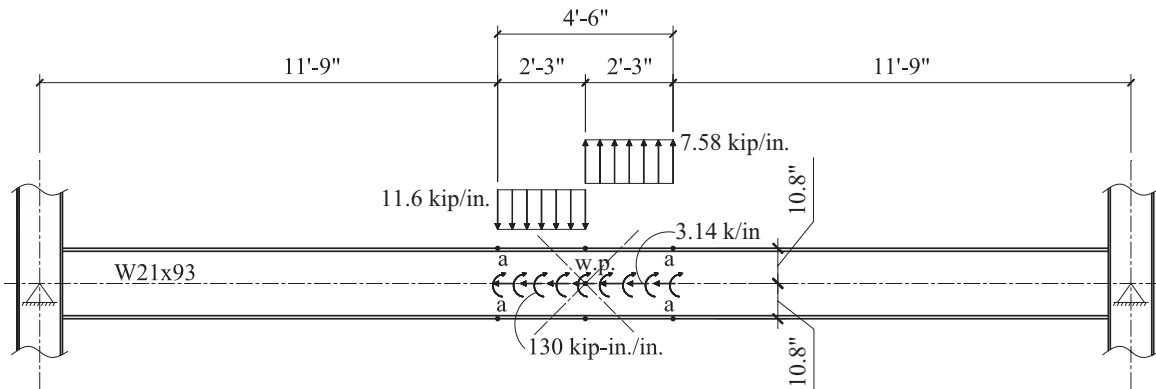
Therefore, the symbiotic method will produce a slightly smaller (very slight difference) beam moment than the current beam designer's method which neglects the local effect. Note that the beam designer used an approximate gusset length of 56.0 in.—2 in. longer than the 54.0 in. used by the connection designer. It is important however, to recognize that neglecting the local effects when determining beam shear will still produce a very unconservative estimate of beam shear. The beam loading for the buckling and post-buckling load cases are shown in Figures 12 and 13, respectively.

Beam Shear and Moment—Current Beam Designer's Method

With this method, the span of the beam and the location of the work point are considered; local effects from the connection are not considered.



(a) Uniformly distributed beam loading



(b) Statically equivalent net beam loading

Fig. 13. Beam loading for post-buckling load case—symbiotic method.

The total summation of the vertical components of the brace forces is treated as a concentrated load acting on the beam at the work point. For this example, the work point is located at mid-span of the beam, so beam shear and moment will be distributed using the following equations. In the following equations, x_1 and x_2 are measured starting from the left beam end and the location of the work point, respectively:

$$R_1 = R_2 = \frac{-(\sum V)_T}{2}$$

$$V(x_1) = R_1$$

$$V(x_2) = -R_2$$

$$M(x_1) = R_1 x_1$$

$$M(x_2) = R_1 a - R_2 x_2$$

Beam Shear and Moment—Current Connection Designer’s Method

With this method, the span of the beam and the location of the work point are not considered; local effects from the connection are considered. Regardless of the unbalanced vertical load, this method assumes that beam shear and moment outside of the connection region are zero.

The beam shear and moment distribution will be as shown in Figure 3b; constant shear with linearly distributed moment acting on the along the middle half of the gusset.

Buckling load case:

$$\begin{aligned} V &= \frac{2[(M_{a-a})_t + (M_{a-a})_b]}{L_g} \\ &= \frac{2(3,078 \text{ kip-in.} + 5,735 \text{ kip-in.})}{54.0 \text{ in.}} \\ &= 326 \text{ kips} \end{aligned}$$

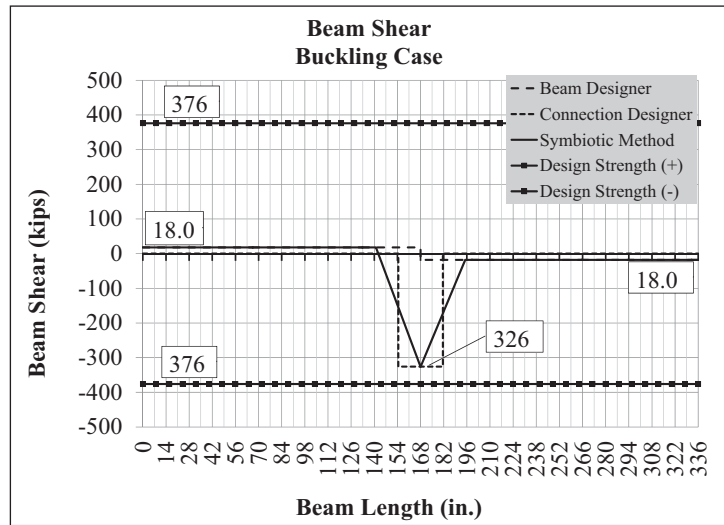
$$\begin{aligned} M &= \frac{(M_{a-a})_t + (M_{a-a})_b}{2} \\ &= \frac{3,078 \text{ kip-in.} + 5,735 \text{ kip-in.}}{2} \\ &= 4,407 \text{ kip-in.} \end{aligned}$$

Post-buckling load case:

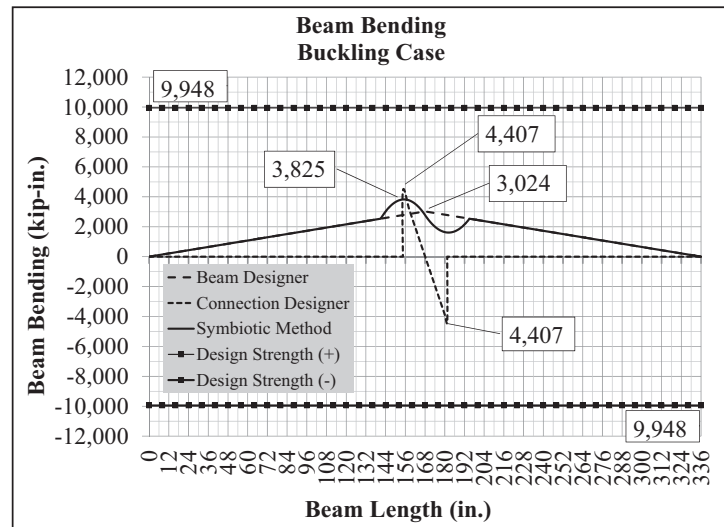
$$\begin{aligned} V &= \frac{2[(M_{a-a})_t + (M_{a-a})_b]}{L_g} \\ &= \frac{2(2,571 \text{ kip-in.} + 4,433 \text{ kip-in.})}{54.0 \text{ in.}} \\ &= 260 \text{ kips} \end{aligned}$$

$$\begin{aligned} M &= \frac{(M_{a-a})_t + (M_{a-a})_b}{2} \\ &= \frac{2,571 \text{ kip-in.} + 4,433 \text{ kip-in.}}{2} \\ &= 3,502 \text{ kip-in.} \end{aligned}$$

The beam shear and moment diagrams for the three methods considered in this example problem are shown in Figures 14 and 15 for the buckling and post-buckling loads cases, respectively.

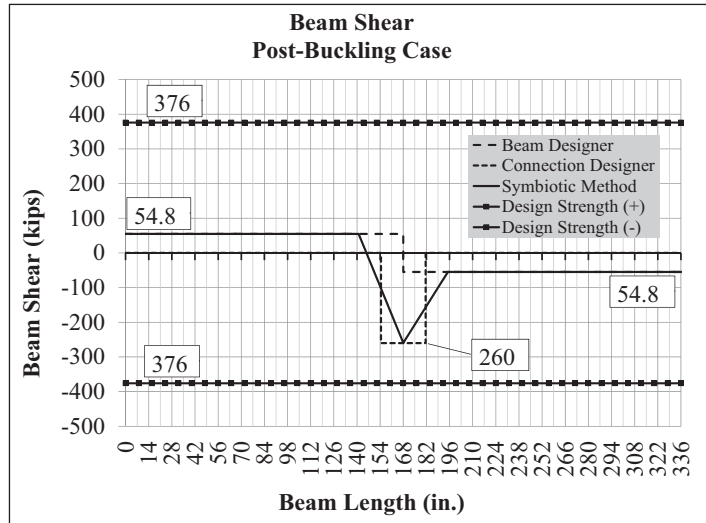


(a) Beam shear

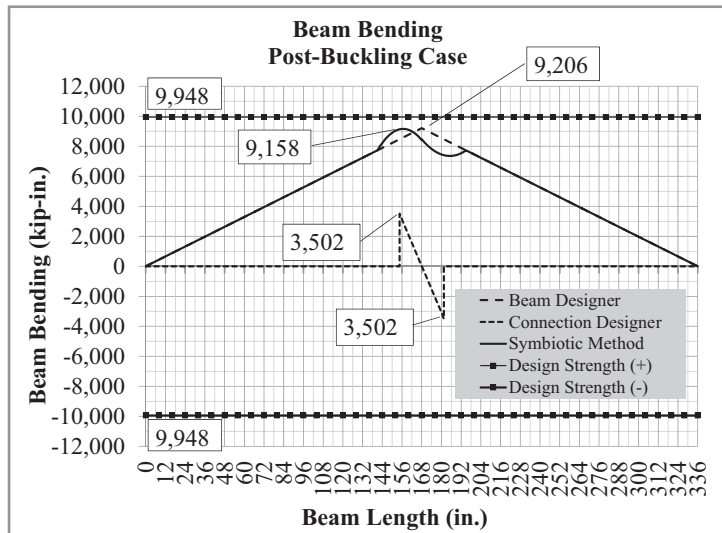


(b) Beam moment

Fig. 14. Beam shear and moment for buckling load case.



(a) Beam shear



(b) Beam moment

Fig. 15. Beam shear and moment for post-buckling load case.

EXAMPLE PROBLEM 2

Figures 14b and 15b show the moment diagrams for Example Problem 1, Part 2, based on the actual connection geometry as shown in Figure 11. Based on the geometry and loading, calculate the equivalent summation of vertical forces, $(\Sigma V)_{T,eq}$, for the buckling and post-buckling cases given in Example Problem 1 (see Figures 11, 12 and 13).

Solution

As can be seen in Figure 11, the eccentricity term, Δ , is zero. Therefore, Equation 53 is used to compute the equivalent unbalanced vertical force, $(\Sigma V)_{T,eq}$. As can be seen in Figures 12 and 13, the work point is located at mid-span of the beam, therefore, the position ratio, b/L , is equal to 0.50. Figures 12 and 13 also give the values for the net uniformly distributed moments, q .

For the buckling case, $q = 163$ kip-in./in. and $(\Sigma V)_T = -36.0$ kips. Therefore, Equation 53 gives

$$\begin{aligned}
 (\Sigma V)_{T,eq} &= q \left[\frac{\frac{b}{L} - \sqrt{\frac{b}{L}}}{\frac{b}{L} - \left(\frac{b}{L}\right)^2} \right] \\
 &= 163 \text{ kip-in./in.} \left[\frac{0.50 - \sqrt{0.50}}{0.50 - (0.50)^2} \right] \\
 &= -135 \text{ kips}
 \end{aligned} \tag{53}$$

The absolute value of $(\Sigma V)_T = 36.0$ kips is smaller than the absolute value of $(\Sigma V)_{T,eq} = 135$ kips. Therefore, the chevron effect will dominate the moment demand on the beam. The moment diagrams shown in Figure 14b support this conclusion.

For the post-buckling case, $q = 130$ kip-in./in. and $(\Sigma V)_T = -109.6$ kips. Therefore, Equation 53 gives

$$\begin{aligned}
 (\Sigma V)_{T,eq} &= 130 \text{ kip-in./in.} \left[\frac{0.50 - \sqrt{0.50}}{0.50 - (0.50)^2} \right] \\
 &= -108 \text{ kips}
 \end{aligned}$$

The absolute value of $(\Sigma V)_T = 109.6$ kips is larger than the absolute value of $(\Sigma V)_{T,eq} = 108$ kips. Therefore, the chevron effect analysis will produce a beam moment smaller than what would be calculated using the classic Pab/L analysis. However, the two values are very close, therefore the moment calculated using the symbiotic method should be only slightly smaller than that computed using the beam designer's method (Pab/L). The moment diagrams shown in Figure 15b support this conclusion; the symbiotic moment is 9,158 kip-in. as compared to the Pab/L moment equal to 9,206 kip-in.

EXAMPLE PROBLEM 3

Figures 16 and 17 show a braced frame elevation and corresponding gusset-to-beam interface forces. The total unbalanced load, $(\Sigma V)_T$, is -112 kips. The total moment, M_T , is 10,203 kip-in. Referring to Figure 16, it can be seen that Δ is nonzero and that the work point is not located at mid-span of the beam. Figure 18 shows the beam moment diagram. Using the information given in Figures 16, 17 and 18:

1. Use Equation 52 to determine if the chevron effect will dominate the maximum beam moment. That is, compare the calculated $(\Sigma V)_{T,eq}$ from Equation 52 to the actual $(\Sigma V)_T$.
2. Use Equation 47 to determine if the chevron effect will dominate the maximum beam moment. That is, compare the calculated $L_{g,eq}$ from Equation 47 to the actual L_g .
3. Calculate the maximum beam moments, $M(x_1)_{max}$ and $M(x_2)_{max}$, evaluate the second derivatives for each region, and compare to the beam moment diagram shown in Figure 18.

Solution

Part 1

Equation 52 is a function of the b/L and Δ/L_g ratios. Those ratios are

$$\frac{b}{L} = \frac{204 \text{ in.}}{336 \text{ in.}} = 0.6071$$

$$\left(\frac{b}{L}\right)^2 = (0.6071)^2 = 0.3686$$

$$\frac{\Delta}{L_g} = \frac{-4.50 \text{ in.}}{57.0 \text{ in.}} = -0.07894$$

$$\left(\frac{\Delta}{L_g}\right)^2 = (-0.07894)^2 = 0.006233$$

To simplify the number crunching required in Equation 52, the following terms within Equation 52 will be calculated and then substituted into the equation:

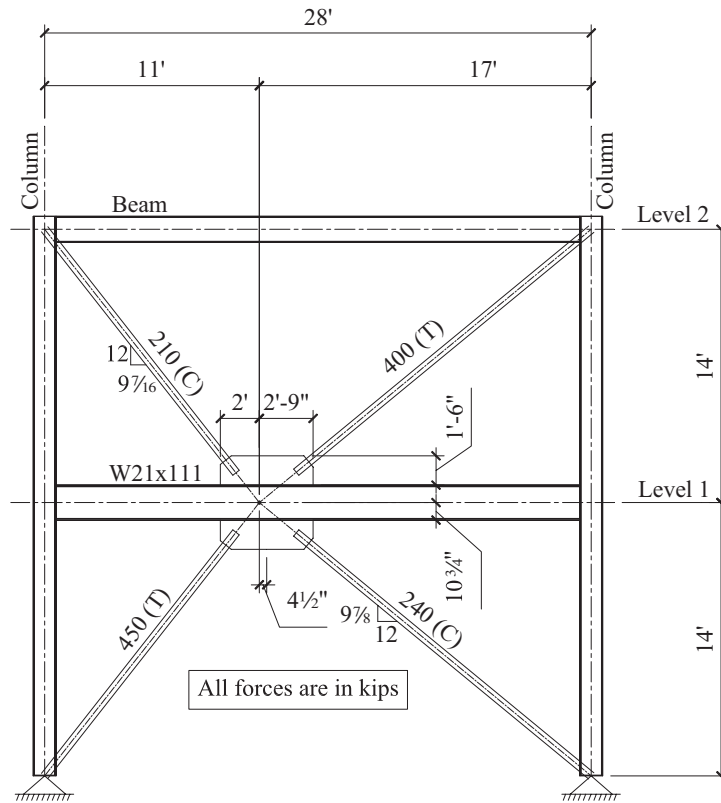


Fig. 16. Frame elevation, loading and connection geometry.

$$\frac{b}{L} + \frac{4\Delta}{L_g} \left(\frac{b}{L} \right) = 0.6071 + (4)(-0.07894)(0.6071)$$

$$= 0.4154$$

$$\left(\frac{b}{L} \right)^2 \left(\frac{8\Delta}{L_g} + \frac{16\Delta^2}{L_g^2} \right) = (0.3686)[(8)(-0.07894) + (16)(0.006233)]$$

$$= -0.1960$$

$$\frac{b}{L} \left(1 - \frac{2\Delta}{L_g} - \frac{8\Delta^2}{L_g^2} \right) = (0.6071)[1 - (2)(-0.07894) - (8)(0.006233)]$$

$$= 0.6727$$

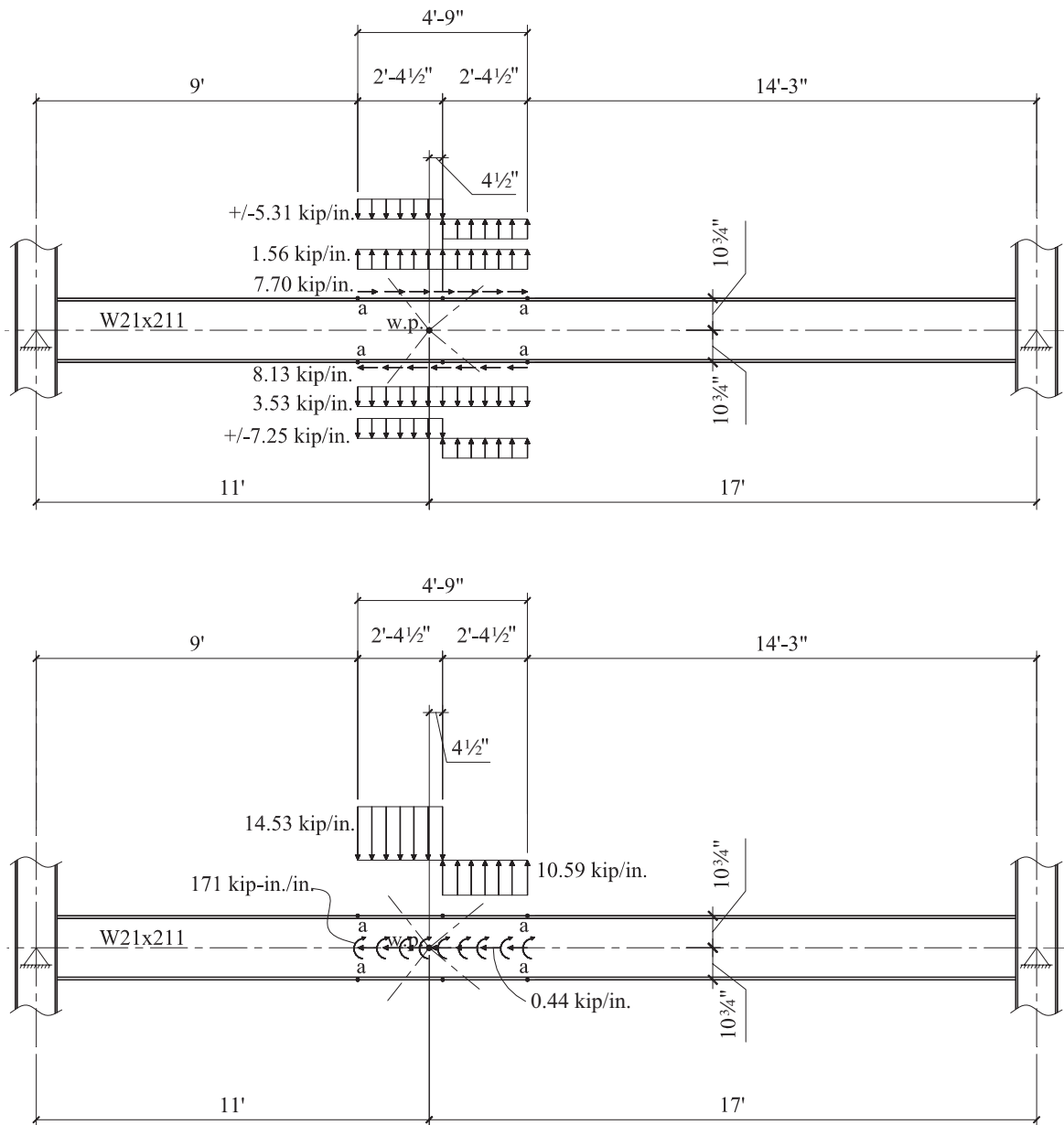


Fig. 17. Beam loading.

Equation 52 gives the following:

$$\begin{aligned}
 (\Sigma V)_{T,eq} &= \frac{q \left[\frac{b}{L} + \frac{4\Delta}{L_g} \left(\frac{b}{L} \right) \right] - q \sqrt{\left[\left(\frac{b}{L} \right)^2 \left(\frac{8\Delta}{L_g} + \frac{16\Delta^2}{L_g^2} \right) + \left(\frac{b}{L} \right) \left(1 - \frac{2\Delta}{L_g} - \frac{8\Delta^2}{L_g^2} \right) \right]}{\left(\frac{b}{L} \right) \left(1 - \frac{2\Delta}{L_g} - \frac{8\Delta^2}{L_g^2} \right) - \left(\frac{b}{L} \right)^2} \\
 &= \frac{(171 \text{ kip-in./in.})(0.4154) - (171 \text{ kip-in./in.})\sqrt{-0.1960 + 0.6727}}{0.6727 - 0.3686} \\
 &= -154 \text{ kips}
 \end{aligned}
 \tag{52}$$

The magnitude of the total unbalanced force, $(\Sigma V)_T$, for this problem is 112 kips. Comparing this magnitude of load to the magnitude of the equivalent unbalanced force, $(\Sigma V)_{T,eq}$ gives

$$|(\Sigma V)_{T,eq}| = 154 \text{ kips} > |(\Sigma V)_T| = 112 \text{ kips}$$

Therefore, the chevron effect will dominate the beam moment. Referring to Figure 18, it can be seen that Equation 51 accurately predicts this.

Part 2

Equation 47 is a function of b/L ratios as well as M_T and $(\Sigma V)_T$. The (b/L) , $(b/L)^2$ and $(b/L)^3$ ratios are 0.607, 0.369 and 0.224, respectively. The variables M_T and $(\Sigma V)_T$ were given as 10,203 kip-in and -112 kips, respectively. The square root of the discriminant, η , is

$$\begin{aligned}
 \eta &= \sqrt{(\Sigma V)_T^2 \Delta^2 \left[\frac{b}{L} - \left(\frac{b}{L} \right)^2 \right] + (\Sigma V)_T M_T \Delta \left[-8 \left(\frac{b}{L} \right)^3 + 10 \left(\frac{b}{L} \right)^2 - 2 \left(\frac{b}{L} \right) \right] + M_T^2 \left(\frac{b}{L} \right)} \\
 &= \sqrt{(-112 \text{ kips})^2 (-4.50 \text{ in.})^2 [0.607 - 0.369] + (-112 \text{ kips})(10,203 \text{ kip-in.})(-4.50 \text{ in.}) [-8(0.224) + 10(0.369) - 2(0.607)] + (10,203 \text{ kip-in.})^2 (0.607)} \\
 &= 8,171 \text{ kip}^2\text{-in.}^2
 \end{aligned}
 \tag{47b}$$

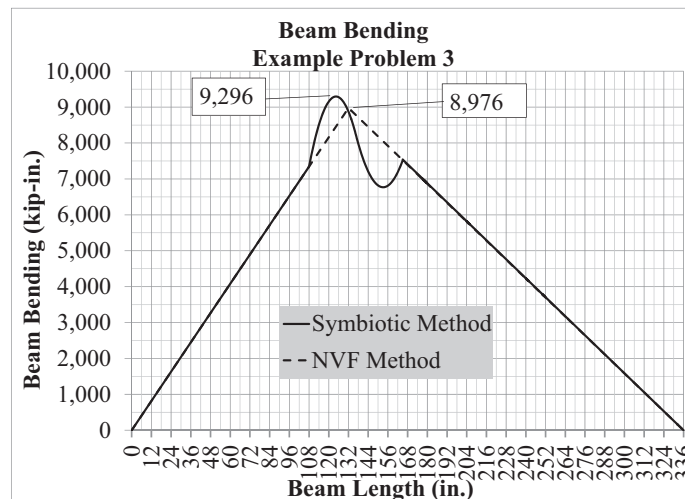


Fig. 18. Beam moment diagram for Example Problem 3.

$$\begin{aligned}
 L_{g,eq} &= \frac{M_T \left(\frac{b}{L} \right) - \eta}{(\Sigma V)_T \left[\frac{b}{L} - \left(\frac{b}{L} \right)^2 \right]} & (47a) \\
 &= \frac{(10,203 \text{ kip-in.})(0.607) - 8,171 \text{ kip}^2\text{-in.}^2}{(-112 \text{ kips})(0.607 - 0.369)} \\
 &= 74.2 \text{ in.} > L_g = 57.0 \text{ in.}
 \end{aligned}$$

Therefore, the chevron effect will dominate the beam moment relative to the Pab/L moment. The moment diagrams shown in Figure 18 support this result.

Part 3

As can be seen in Figure 16, the w_l and w_r terms are negative and positive, respectively. Additionally, the moments are in the positive region. Therefore, the second derivative of the $M(x_1)$ equation gives a maximum moment, and the second derivative of the $M(x_2)$ equation gives a minimum. The moment diagram shown in Figure 17 supports this conclusion.

FURTHER DISCUSSION

The procedures presented in this paper provide a general solution that both beam designers and connection designers can use in a consistent manner to evaluate beam shear and moment in beams of V-type and inverted V-type braced frames. Beyond the general need to have a consistent analysis procedure, the proposed procedure also has the advantage that the beam designer can account for brace connection geometry at the time the beam is sized in a manner that will ensure that beam web and flange reinforcement is not found to be required during the connection design phase.

The example problem used to illustrate the application of the proposed procedure is illustrated in the context of a seismic system using the mechanistic analysis required in the AISC *Seismic Provisions* (2016) for special concentrically braced frames. It is important to recognize that the chevron effect has an impact on beams in systems designed for low seismic and wind requirements. Posted brace forces that are used for design in low seismic and wind applications often result in an unbalanced vertical force—usually relatively small unbalanced vertical loads. As has been shown in this paper, if a beam is sized for beam shear and moment strength for relatively small unbalanced vertical loads using the current beam and connection designer’s methods, the beam shear and moment arising from the chevron effect in the connection region can be significantly underestimated, leading to expensive beam web and flange reinforcement. The proposed symbiotic method will minimize, if not eliminate, the need for such reinforcement.

Several assumptions (see the “Symbiotic Analysis Model” section) are made in regard to connection geometry, as

discussed at the beginning of this paper. It is also important to recognize that beam shear and moment can be very sensitive to beam span, location of work point, brace bevel, and brace loading. The proposed procedures are based on these assumptions and several checks are provided to ensure that the equations that have been derived apply to the problem being considered. When these assumptions are not valid, designers must take care to return to engineering fundamentals and first principles to solve that particular problem.

CONCLUSIONS

The methods used by beam designers and connection designers to evaluate beams in V-type or inverted V-type frames are not consistent. Beam designers consider beam span and work point location but ignore the effects of the connection geometry (chevron effect), while connection designers consider the effect of the moment acting on the gusset–beam interface(s) but neglect the unbalanced vertical load as well as the beam span and work point location. The symbiotic method proposed in this paper provides a consistent analysis model that can be used by beam and connection designers alike.

This paper provides beam and connection designers with methods for evaluating whether the chevron effect will dominate the moment demand on the beam and also to determine whether the current methods being used are conservative. Equation 47 can be used to evaluate a beam for a given set of brace forces and frame geometry to determine a gusset length interface that will reduce the chevron effect relative to the Pab/L moment, which is more likely useful

to a connection designer for a specific case. Equations 50 and 51 can be used to evaluate a beam for a given beam span and work point location, combined with approximated gusset lengths, $L_{g,app}$, and half-beam depths, $e_{b,app}$ (see Equations 42 and 43), to determine at what level of unbalanced vertical force the chevron effect will dominate beam demand relative to a Pab/L moment, which is more likely useful to a beam designer to use in a more general sense when evaluating multiple joints in a frame.

When the chevron effect dominates, the current analysis procedure used by beam designers and connection designers can significantly underestimate beam shear and moment in the balanced case and when a relatively small unbalanced vertical load is present. In this case, the beam can be significantly undersized for the demands imposed on the beam by the chevron effect. When the unbalanced vertical load is relatively large, the symbiotic method potentially provides a smaller beam moment demand, which may lead to a lighter beam relative to one required using the methods currently used by beam and connection designers.

ACKNOWLEDGMENTS

The authors would like to thank Mr. Joshua R. Buckholt, P.E., S.E., for his comments during the review process of this paper.

SYMBOLS

H_1	Horizontal component of force in brace 1, kips	$M_{max,local}$	Maximum beam moment when local effects are considered, kip-in.
H_2	Horizontal component of force in brace 2, kips	$M_{max,unbal}$	Maximum beam moment when local effects are not considered, kip-in.
H_{a-a}	Horizontal (shear) force acting at the gusset-to-beam interface, kips	M_T	Sum of moments at top and bottom gusset interfaces, $(M_{a-a})_t$ and $(M_{a-a})_b$, kip-in.
H_{bi}	Horizontal (normal) force acting on the critical vertical section of the gusset, kips	$M_{u,max}$	Maximum required (design) flexural strength, kip-in.
L_1	Horizontal distance from the left edge of the gusset to the work point, in.	$M(x_1)$	Beam moment as a function of x_1 , kip-in.
L_2	Horizontal distance from the right edge of the gusset to the work point, in.	$M(x_2)$	Beam moment as a function of x_2 , kip-in.
L	Span of frame beam, in.	N_{eq}	Couple of the moment, M_{a-a} , kip-in.
L_g	Contact length of the gusset-to-beam interface, in.	$P_i(T)$	Tension brace force, kips
$L_{g,app}$	Approximation of length of gusset, L_g , in.	$P_i(C)$	Compression brace force, kips
$L_{g,eq}$	Minimum gusset length required such that the chevron effect does not dominate, in.	P_1	Axial force in brace 1, kips
M_{a-a}	Moment acting at the gusset-to-beam interface, kip-in.	P_2	Axial force in brace 2, kips
M_{max}	Maximum required beam moment, kip-in.	R_1	Left beam end reaction, kips
		$R_{1,eq}$	Left beam end reaction that identifies the magnitude of an unbalanced force at which local effects dominate beam moment demands, kips
		V_1	Vertical component of the force in brace 1, kips
		V_2	Vertical component of the force in brace 2, kips
		V_{a-a}	Vertical (normal) force acting at the gusset-to-beam interface, kips
		V_{max}	Maximum required beam shear, kips
		$V_{u,max}$	Maximum required (design) shear strength, kips
		$V(x_1)$	Beam shear as a function of x_1 , kips
		$V(x_2)$	Beam shear as a function of x_2 , kips
		Z	Plastic section modulus, in. ³
		a	Distance from left beam support to location of work point, in.
		a'	Distance from left beam support to left edge of gusset, in.
		b	Distance from work point to right beam support, in.
		d	Depth of frame beam, in.
		e_b	Perpendicular distance from the gusset interface to the gravity axis of the frame beam, in.
		$e_{b,app}$	Approximation of length of half-depth of the frame beam, in.
		h	Vertical dimension of the gusset, in.

q	Net uniformly distributed moment, kip-in.
w_l	Net uniformly distributed transverse load on left half of gusset, kip/in.
w_r	Net uniformly distributed transverse load on right half of gusset, kip/in.
w.p.	Brace work point
Δ	Horizontal misalignment between the work point and the centroid of the gusset-to-beam interface, in.
ΔM_{local}	Change in beam moment from the left edge of the gusset to location of maximum moment when local effects are considered, kip-in.
ΔM_{unbal}	Change in beam moment from the left edge of the gusset to location of maximum moment when local effects are not considered, kip-in.
ΣV_i	Summation of vertical brace force components (unbalanced vertical force), kips

REFERENCES

- AISC (2016), *Seismic Provisions for Structural Steel Buildings*, ANSI/AISC 341-16, American Institute of Steel Construction, Chicago, IL.
- AISC (2017), *Steel Construction Manual*, 15th Ed., American Institute of Steel Construction, Chicago, IL.
- Fortney, P.J. and Thornton, W.A. (2015), "The CHEVRON EFFECT—Not an Isolated Problem," *Engineering Journal*, AISC, Vol. 52, No. 2, pp. 125–163.